Advancing Organic Solar Cells with Density Functional Theory:

A Comprehensive Review of Computed Properties and Applications

Nathália M. P. Rosa[a] and Itamar Borges, Jr.[a,]*

[a] *Departamento de Química, Instituto Militar de Engenharia (IME), Praça General Tibúrcio 80, Rio de Janeiro, Brazil;*

* itamar@ime.eb.br (e-mail of the corresponding author)

Abstract

Context

Organic solar cells (OSCs) represent a promising renewable energy technology due to their flexibility, low production cost, and environmental sustainability. To advance OSC efficiency and stability, Density Functional Theory (DFT) has emerged as a powerful computational tool, enabling the prediction and optimization of critical properties at the molecular and device levels. This review highlights the key properties of bulk heterojunction solar (BHJ) solar cells and dye-sensitized solar cells (DSSCs) that can be accurately computed using DFT, including **electronic structure properties (**HOMO-LUMO energy levels, bandgap energies, and exciton binding energies, which influence charge separation and transport); **optical properties (**absorption spectra and light-harvesting efficiency, essential for maximizing photon capture); **charge transport properties (**reorganization energies, electron, and hole mobilities, and charge transfer rates that govern carrier dynamics within devices); **interfacial properties (**energy alignment at donor-acceptor interfaces, contributing to efficient charge separation and minimizing recombination) and **chemical reactivity descriptors (**ionization potential, electron affinity, chemical hardness, and electrophilicity, which facilitate material screening for OSC applications). We also show how to compute the power conversion efficiency (PCE) of OSCs from DFT.

Methods

The review also discusses the importance of selecting appropriate exchange-correlation functionals and basis sets to ensure the accuracy of DFT predictions. By providing reliable computational insights, DFT accelerates the rational design of OSC materials, guiding experimental efforts and reducing resource demands. This work underscores DFT's pivotal role in optimizing OSC performance, fostering the development of next-generation photovoltaic technologies.

Keywords: Organic Solar Cells (OSCs); Bulk heterojunction (BHJ) solar cells and Dye-sensitized solar cells (DSSCs); Density Functional Theory (DFT); Optoelectronic properties; Charge transport dynamics, Exciton Dissociation, Energy level alignment.

ORCID ID:

Nathália M. P. Rosa - 0000-0002-3915-0036

Itamar Borges Jr - 0000-0002-8492-1223

Author Contributions

Nathália M. P. Rosa – Data curation, visualization, writing – review, and editing.

Itamar Borges Jr – Data curation, visualization, conceptualization, methodology, funding acquisition, project administration, resources, supervision, writing – review and editing.

Acknowledgements

I. B. thanks the Brazilian agencies CNPq (Grant numbers 304148/2018-0 and 409447/2018-8) and FAPERJ (Grant number E26/201.197/2021) for funding this research. Nathália M. P. Rosa thanks FAPERJ (grant number E-26/204.294/2024) for a post-doctoral scholarship. Support for this research also came from the National Institute of Science and Technology on Molecular Sciences (INCT-CiMol) grant CNPq 406804/2022-2, and Nano Network grant FAPERJ E-26/200.008/2020.

Introduction

The availability of energy has been a transformative factor in human history. Given the substantial increase in global consumption in recent years, transitioning to a more sustainable energy matrix has become crucial to mitigate climate change and ensure global energy security (**Fig.1**) [1–3]. According to the 2024 "Statistical Review of World Energy," global primary energy consumption reached a new record high for the second consecutive year. Renewable energy generation saw significant growth, with a 13% increase in electricity production from renewable sources such as solar and wind [3–6]. Consequently, much research has focused on developing clean fuel technologies and alternative energy sources [6]. In this context, research on solar energy has become particularly attractive, given the abundant daily influx of sunlight reaching the Earth's surface, which far exceeds the planet's annual energy needs [2, 6].

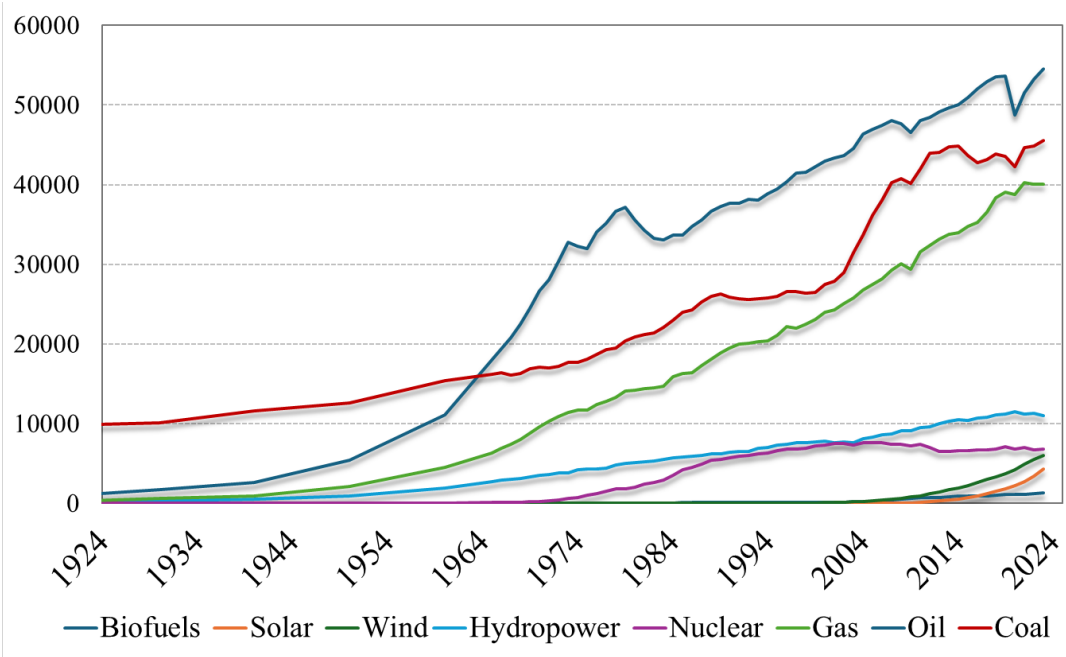

Fig. 1. Global primary energy consumption in the last 100 years by source type [3].

Solar energy is an attractive power source, the most abundant renewable resource available, and can be harnessed directly and indirectly. The solar radiation that reaches

the Earth's surface amounts to approximately 3400000 exajoules (EJ) per year, which surpasses all estimated non-renewable energy resources, including fossil fuels and nuclear energy [7]. Considering the vast potential of solar energy, photovoltaic technologies have evolved significantly over different technological generations, with each advancement aiming for greater efficiency, flexibility, and cost reduction, from conventional silicon cells to modern third-generation organic cells, such as bulk heterojunction (BHJ) and dye-sensitized solar cells (DSSCs).

Photovoltaic devices directly convert solar energy into electricity and encompass many photovoltaic cell technologies [8–10]. Depending on the component materials, these technologies are classified into three generations. First-generation photovoltaic systems utilize crystalline silicon technology, already commercially available. Second-generation systems are based on thin-film photovoltaic technologies, which cells are deposited on flexible substrates, allowing for greater applicability on irregular surfaces. Finally, third-generation photovoltaic systems include organic photovoltaic technologies, still are not widely commercialized [8, 9].

Organic optoelectronic materials have been known since the 1910s. Interest in these materials grew significantly during the 1960s and 1970s driven by the discovery of electroluminescence in anthracene crystals, reported by Pope in 1963 [11, 12] and by Helfrich and Schneider in 1965 [13], and with the discovery that π-conjugated polymers, such as hydrocarbon chains with alternating bonds, can achieve high conductivities when doped [14–18]. Currently, these materials are widely studied for applications in electronic and optoelectronic devices, such as organic light light-emitting diodes (OLEDs), organic solar cells, organic transistors, and sensors [19–25]. Organic photovoltaic materials used in organic solar cells (OSCs) for light absorption and charge transport are based on conjugated organic semiconducting molecules, such as oligomers and polymers [26, 27]. These devices are manufactured more simply and cost-effectively, and although OSC efficiency is still not comparable to traditional photovoltaic technologies, it has improved significantly in recent years [28–34]. OSCs are typically composed of thin films of electron donor (D) and acceptor (A) materials sandwiched between electrodes, one of which must be transparent to allow light to enter [35–37]. Due to the low dielectric constant of organic materials, photoexcitation generates tightly bound excitons (electron-

hole pairs), which must be dissociated into free charge carriers, a process that occurs at the D–A interface [26, 38]. The electron and hole carriers are then transported to the electrodes, generating an electric current. However, charge dissociation and transport are limited by the short diffusion length of excitons in these materials [39].

Although OSC development has made significant advancements, their efficiency is still lower than that of traditional technologies, such as crystalline silicon. Additionally, the degradation of organic materials when exposed to light and oxygen can drastically limit their lifespan, thus requiring improvements in material's chemistry [40–43]. Devices with efficiencies exceeding 15% have already been reported [34, 44–46]. The evolution of energy conversion efficiency in solar cells in recent years is summarized in **Fig. 2**, based on data extracted from annual solar cell efficiency tables, listing the highest confirmed efficiencies [47–65]. Scaling up production for large-scale manufacturing also presents a challenge, as while OSCs can be produced more economically through methods like roll-to-roll printing, ensuring uniformity and quality across large surfaces remains a technological barrier [43, 66]. These challenges highlight the need for new approaches, including using theoretical calculations to optimize molecular design and improve the understanding of degradation and charge transport mechanisms.

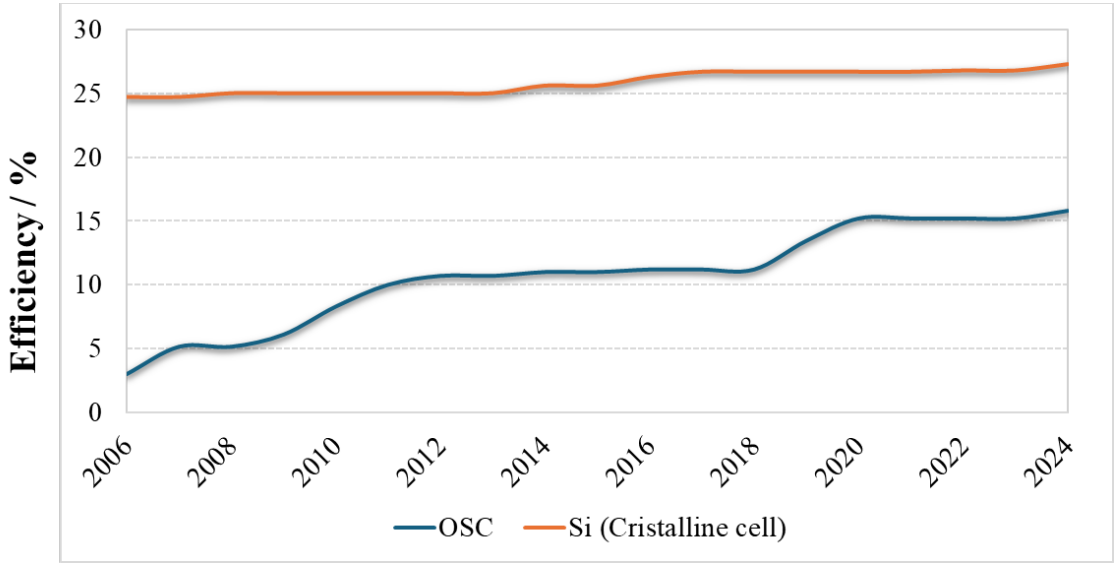

Fig. 2. Reports on energy conversion efficiencies of single-junction organic solar cells and crystalline silicon [47–65].

Density Functional Theory (DFT) calculations play a fundamental role in predicting and evaluating the optoelectronic properties of materials for applications in photovoltaic devices, such as BHJs solar cells and DSSCs [24, 25, 67–72]. DFT provides detailed insights into the electronic structure and optical absorption properties, which are essential for optimizing the performance of these materials in light-harvesting and charge transport processes [73–75]. Compared to experimental methods, DFT offers a more cost-effective and efficient alternative, enabling the rapid screening of potential candidates [75, 76]. Since the synthesis and experimental testing of new materials can be time-consuming and expensive, DFT can be a valuable tool to guide experiments by identifying the most promising candidates in advance, reducing costs and saving time. As a result, DFT can accelerate the development process, optimize resource use, and expand the ability to explore a broader range of materials for photovoltaic applications.

Given the growing interest in organic optoelectronic materials due to their versatility and potential to revolutionize various technologies, from lighting and energy-harvesting devices to sensors and transistors, we present a comprehensive review of the use of quantum mechanical calculations to predict and analyze the optoelectronic properties of organic materials, with a focus on their applications in OSCs.

Basic working principle of an organic photovoltaic (OPV) device

The fundamental operation principle of an organic photovoltaic device (OPV) is the direct conversion of solar energy into electricity through semiconducting organic materials [77]. These devices consist of an active layer, usually composed of an electron donor and acceptor material, sandwiched between two electrodes, one transparent to allow sunlight to enter [77–79]. When light hits the device, it excites electronically the organic molecules in the active layer, generating tightly bound electron-hole pairs (excitons). These excitons are separated into free charges at the interface between the donor and acceptor materials, allowing electrons to be transported to one electrode and holes to the other, generating an electric current. The efficiency of this process depends on several factors, including the exciton dissociation capability and the effective transport of charges to the electrodes [78–81].

Organic electronic materials are conjugated polymers in which optical absorption and charge transport are governed by partially delocalized π electrons [80]. This property makes them promising candidates for various photovoltaic applications [24, 67, 68, 82–84]. Concerning OSCs, the BHJ-type combines donor and acceptor materials in an interpenetrating active layer, maximizing the interface area for exciton dissociation and facilitating charge transport, which results in higher energy conversion efficiency [85]. The DSSC-type, on the other hand, utilizes photosensitive dyes to capture light, enabling efficient charge separation at the dye-semiconductor interface [86, 87]. Both technologies offer flexibility, low production costs, and the potential for large-scale manufacturing, positioning them as sustainable and promising alternatives for solar energy generation [86, 88]. Therefore, BHJs and DSSCs can be used on flexible surfaces and portable devices, expanding their potential use in different scenarios.

Bulk heterojunction (BHJ) organic solar cells

The operation of BHJ solar cells relies on the architecture of their active layer. The active layer of a BHJ (**Fig. 3a**) consists of a highly interconnected blend of donor and acceptor materials, forming an interpenetrating amorphous network that maximizes the interface between these components. This architecture enhances exciton dissociation efficiency, generating more significant electrical current. Despite ongoing challenges related to efficiency and stability, BHJ-type OSCs have shown significant potential to emerge as a competitive alternative to conventional photovoltaic technologies [43, 85, 89].

The operation of a BHJ solar cell involves four main steps (**Fig. 3b**): (1) light absorption, where electron-donor molecules absorb photons incident on the active layer; (2) formation of tightly bound excitons in the donor material; (3) dissociation of these excitons at the interface between the donor (D) and electron acceptor (A) materials in an electronic charge transfer state, resulting in free electrons and holes; and (4) charge transport taking place in an electronic charge separation state, where the electrons are conducted through the acceptor material to the cathode, while the holes are transported

through the donor material to the anode. Once the electrons and holes reach their respective electrodes, an electric current is generated in the external circuit [43, 90–92].

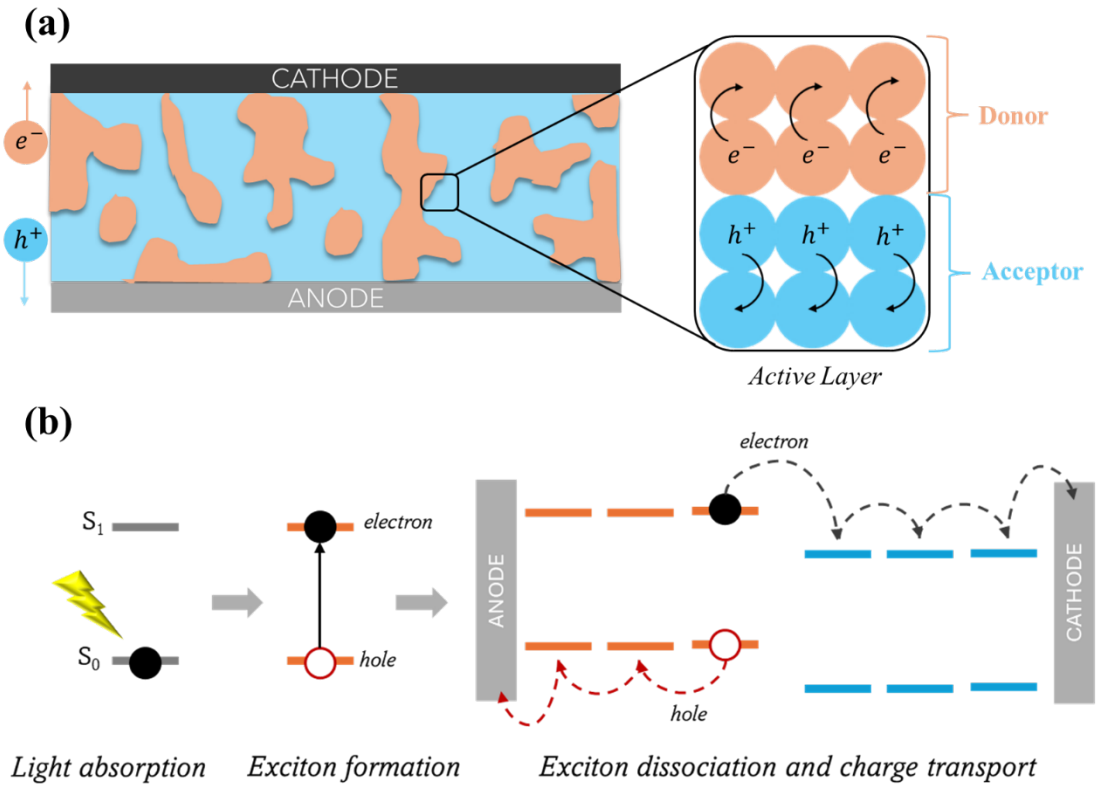

Fig. 3. (a) Active layer of a bulk heterojunction (BHJ) organic solar cells; (b) Diagram illustrating the operating mechanism of a BHJ cell, highlighting the processes of light absorption, exciton generation, charge dissociation at the donor/acceptor interface, and charge transport to the electrodes.

To achieve high power conversion efficiency (PCE) in BHJ solar cells, the active layer must have a sufficiently broad absorption spectrum in the wavelength range between 250 nm (4.96 eV) and 3000 nm (0.413 eV) [93] of the solar spectrum to maximize the capture of photons from sunlight. Additionally, the active layer should present appropriate energy levels in the highest occupied molecular orbitals (HOMO) and the lowest unoccupied molecular orbitals (LUMO) for both the donor and acceptor materials. After photon absorption, an electron is excited from the donor's HOMO to its LUMO and then transferred to the acceptor's LUMO, which has a lower energy level (**Fig. 3b**) [43, 89]. For this process to be efficient, an appropriate energy offset between the donor's LUMO and the acceptor's LUMO, typically in the range of 0.1–1.4 eV, is crucial to overcome the

Coulomb attraction and ensure exciton dissociation into free charges [43, 94]. Furthermore, the efficiency of a solar cell is directly influenced by the open-circuit voltage (V_{OC}), which is linearly related to the energy difference between the donor's HOMO and the acceptor's LUMO [89, 95]. Thus, the more significant this difference, the higher the theoretically-predicted value of V_{OC}. However, the overall device efficiency also depends on minimizing energy losses through processes as charge recombination and internal resistance, to achieve optimized performance [95]. The active layer must also exhibit good charge mobility, which promotes efficient exciton separation and facilitates the effective transfer of electrical charges [24, 84, 96–99].

Dye-sensitized solar cell (DSSC)

DSSCs have become a promising alternative for photovoltaic solar energy generation [86, 87, 100, 101]. This is due to the exceptionally low-cost materials, mechanical flexibility, ease of fabrication and assembly, and environmentally friendly nature [102–105]. The basic working principle of a dye-sensitized solar cell (**Fig. 4a**) involves a photosensitive dye adsorbed onto the surface of a semiconductor material, typically titanium dioxide (TiO_2) or Zinc Oxide (ZnO) [106–108]. When sunlight strikes the device, photons are absorbed by the dye, promoting electrons from the ground state to an excited state. These excited electrons are quickly injected into the conduction band of the semiconductor. In contrast, the dye, which has lost an electron, is regenerated by an electrolyte in the cell, usually composed of the I_3^-/I^- redox couple [109–112]. The semiconductor transports the injected electrons to the conducting electrode, known as the photoanode, generating an electric current. Simultaneously, the electrolyte completes the cycle by transferring electrons to regenerate the dye, thus closing the circuit. This process, shown in **Fig. 4b**, efficiently converts sunlight into electricity, with the dye absorbing light and generating electrical charges [86, 87, 113, 114].

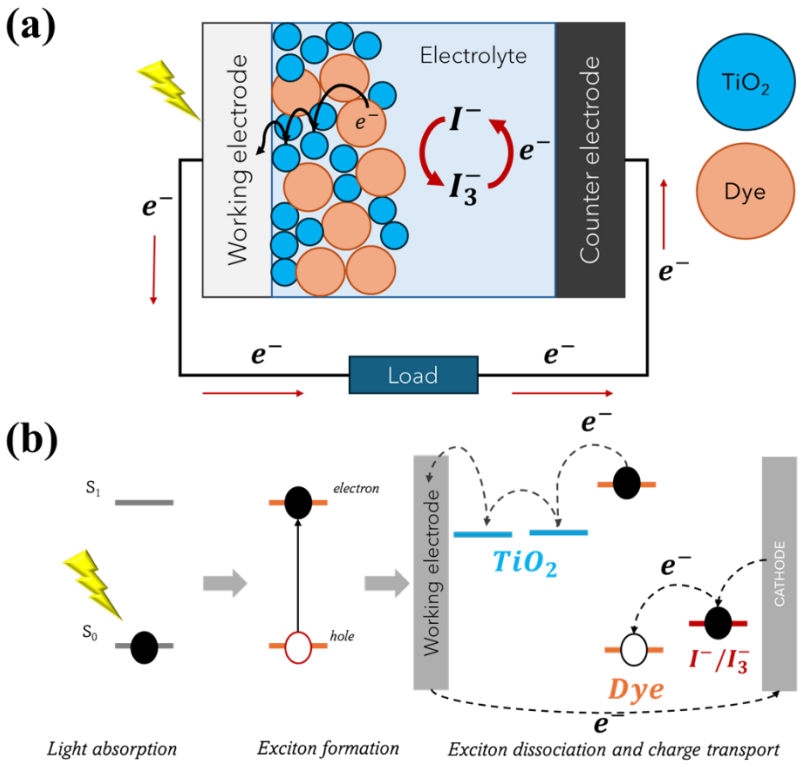

Fig. 4. (a) Operation diagram of the operation of a dye-sensitized solar cell (DSSC) and; (b) Energy level diagram, highlighting the processes of light absorption by the dye, electron injection into the semiconductor, and dye regeneration by the electrolyte.

DFT-based methods for evaluating organic photovoltaic efficiency

DFT can assist in developing materials for organic photovoltaic devices because it provides an efficient and cost-effective way to assess critical properties [24, 25, 67, 68, 115–119]. Through accurate DFT calculations, it is possible to predict and optimize critical characteristics of OPVs, such as light absorption and HOMO-LUMO energy levels, which determine the energy conversion efficiency of the devices [120, 121]. This approach can providew rapid material screening and fine-tuning of properties, reducing the need for extensive experimentation and saving resources. Additionally, DFT provides detailed insights into the electronic structure and behavior of materials at the molecular level, guiding the selection of promising candidates and accelerating the innovation process in third-generation photovoltaic devices.

Evaluation of the performance of organic photovoltaic devices

To theoretically assess the performance of OSCs, it is essential to examine different properties that directly impact their efficiency. Among the key parameters for measuring the efficiency of these devices, the power conversion efficiency (PCE) quantifies the device's ability to convert incident solar energy into electricity. The PCE is influenced by the short-circuit current (J_{sc}), the open-circuit voltage (V_{OC}), and the fill factor (FF). The latter reflects the quality of the cell by indicating internal losses and the efficiency of charge transport [43, 76, 122]. The device's ability to absorb light across different wavelengths is also crucial to maximize J_{sc} and enhances overall performance [43]. Another critical factor is charge mobility, given that high transport and low recombination rates ensure the efficient motion of electrons and holes, contributing to a more significant current generation [123, 124].

Understanding the relationship between the frontier orbital energy levels in donor-acceptor systems is essential because they directly affect the parameters that determine device efficiency. The frontier molecular orbitals, HOMO (Highest Occupied Molecular Orbital) and LUMO (Lowest Unoccupied Molecular Orbital) play a central role in light absorption and charge transfer processes in organic photovoltaic devices, as the energy difference between these levels affects electronic excitation and the efficient conversion of solar energy into electricity. A schematic diagram of the energy levels of a typical donor-acceptor system is shown in

Fig. 5. After photon absorption by the donor material, an exciton is formed. However, due to the low dielectric constant of organic materials, it is difficult to dissociate the strongly electrostatic bound exciton into free charges under normal (ambient) conditions. To overcome this binding energy, acceptor molecules with appropriately aligned HOMO and LUMO levels are required to produce the driving force for the rapid transfer of electrons from the donor to the acceptor. In this way, both the donor and the acceptor can contribute to the absorption spectrum of the solar cell, enhancing its efficiency in light capture and free charge generation.

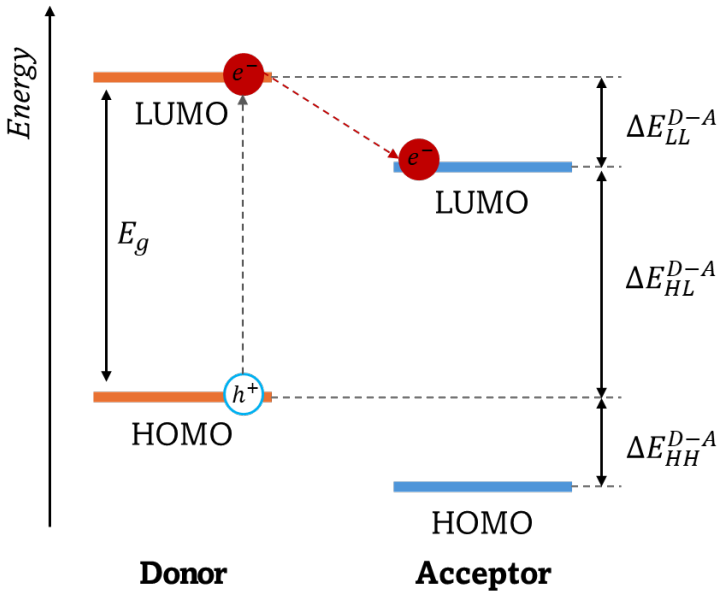

Fig. 5. Energy level diagram of a donor-acceptor system. Upon incidence of light, a hole (h^+) is produced in the ground state and an electron (e^-) is excited. The $e^- - h^+$ pair is an exciton. The energy differences on the right are discussed on the text.

Overall, the design of new donor molecules or materials for OSCs seeks to optimize three key parameters: light harvesting, hole mobility, and PCE. Light harvesting is characterized by the bandgap (E_g), absorption spectrum width, and molecular absorption coefficient [125, 126]. Controlling the bandgap is essential to fine-tune these properties [127, 128] The HOMO-LUMO gap defined in Eq. (1) as the energy difference between the HOMO and LUMO is a fundamental measure of light absorption efficiency in organic materials.

$$E_g = E_{HOMO} - E_{LUMO} \quad (1)$$

A detailed understanding of HOMO-LUMO energy levels, as well as the energy differences between HOMO and HOMO-1 (ΔE_{HOMO}) and LUMO and LUMO+1 (ΔE_{LUMO}) of donor materials is thus essential for refining the design of photovoltaic materials, enabling fine adjustments that directly impact exciton dissociation efficiency and charge transport in devices. Small energy differences between in ΔE_{HOMO} and ΔE_{LUMO} indicate that nearby molecular orbitals can also contribute to exciton formation

and dissociation, as well as to hole and electron transport [127, 128]. In donor molecules with low ΔE_{HOMO} and ΔE_{LUMO}, defined by Eqs. (2) and (3) below, this additional contribution can enhance device efficiency.

$$\Delta E_{HOMO} = E_{HOMO} - E_{HOMO-1} \quad (2)$$

$$\Delta E_{LUMO} = E_{LUMO+1} - E_{LUMO} \quad (3)$$

The alignment of energy levels at donor (D)–acceptor (A) heterojunctions plays a crucial role in the mechanisms of charge generation and recombination in BHJ devices [129, 130]. The energy of the charge transfer state at the donor-acceptor (D/A) interface can be well approximated by the energy difference between the HOMO of the donor and the LUMO of the acceptor, ΔE_{HL}^{D-A}, defined by Eq. (4) below. This difference is widely used to estimate the driving force required for exciton dissociation at the D/A interface, a crucial process for the efficiency of photovoltaic devices. The alignment of the frontier molecular orbital levels at the donor-acceptor interface can be evaluated by the energy difference between the LUMO levels of the donor and acceptor, ΔE_{LL}^{D-A}, defined in Eq. (5). This parameter measures the degree of alignment between the LUMOs, directly influencing the photoelectric efficiency. Excessively high values of ΔE_{LL}^{D-A} indicate significant energy losses at the D/A interface, impairing device performance [24, 127].

$$\Delta E_{HL}^{D-A} = E_{LUMO}^{A} - E_{HOMO}^{D} \quad (4)$$

$$\Delta E_{LL}^{D-A} = E_{LUMO}^{D} - E_{LUMO}^{A} \quad (5)$$

It is also other relations between frontier orbitals in donor and acceptor materials. The energy difference between the HOMO of the donor and acceptor, ΔE_{HH}^{D-A}, defined in Eq. (6), quantify the alignment between the HOMOs of the molecules. A small difference in HOMO energy levels is advantageous for achieving a high open-circuit voltage (V_{OC}), significantly contributing to the overall performance of solar cells. On the other hand, a

larger HOMO offset facilitates more efficient charge separation; as this offset increases, the device's ability to effectively separate charges also improves, which is essential for maintaining high efficiency [131]. Wang and collaborators [132] emphasize that finding the optimal balance in this offset is crucial. A HOMO offset close to 0 eV can result in superior performance in OSCs, characterized by a high open-circuit voltage and an elevated fill factor, suggesting that charge separation reaches its maximum potential when the HOMO offset is carefully optimized [132, 133]. This quantity is relevant for understanding charge transfer and recombination processes at the D/A interface, and it is also a determining factor in optimizing materials for photovoltaic devices [134].

$$\Delta E_{HH}^{D-A} = E_{HOMO}^{A} - E_{HOMO}^{D} \quad (6)$$

The behavior of excitons in donor materials is crucial for understanding charge separation efficiency. In donor materials, electronic excitation by light generates an exciton strongly bound by a Coulombic (i.e., electrostatic) attraction. The exciton binding energy (E_{bind}) is defined as the difference between the fundamental gap (E_{fund}) and the optical gap (E_{opt}), which quantifies this binding energy of the exciton:

$$E_{bind} = E_{fund} - E_{opt} \quad (7)$$

In OSCs, due to the low dielectric constants of organic photoactive materials, E_{bind} can reach values of several tenths of an eV [135–140], making exciton dissociation into free charges extremely challenging in pure materials [141]. Thus, the lower the value of E_{bind}, the more easily the exciton can dissociate. Exciton dissociation into free holes and electrons at donor/acceptor (D/A) interfaces is driven by the energy level offsets between donor and acceptor materials, allowing the excitons to overcome the E_{bind}. Experimental and theoretical studies frequently report E_{bind} values ranging from 0.3 to 1.0 eV in typical materials used in BHJ solar cells and dye sensitizers in DSSCs [138, 142–146]. The fundamental gap, E_{fund}, plays an essential role in calculating the exciton binding energy E_{bind}, as it reflects the energy difference between the adiabatic ionization

potential (IP_a) and the adiabatic electron affinity (EA_a) [143]. The ionization potential is determined by the total energy difference between the ground state and the $N-1$ electronic state, while the electron affinity is given by the energy difference between the N electron ground state and the $N+1$ electronic state. IP_a and EA_a are computed using the adiabatic approach, which optimizes the geometries of the cation and anion separately. The fundamental gap E_{fund} is then given by the energy difference

$$E_{fund} = IP_{(a)} - EA_{(a)} \tag{8}$$

The optical gap E_{opt} of a molecule corresponds to the energy of the lowest allowed electronic transition single photon absorption, often from the ground state S_0 to the first excited state S_1. In this context, the optical gap E_{opt} is the energy difference between the optimized structures of the S_1 and S_0 states, representing the fundamental transition that directly influences the material's light absorption efficiency:

$$E_{opt} = E_{S_1} - E_{S_0} \tag{9}$$

To evaluate the performance of organic photovoltaic devices, calculating the PCE is essential, as it provides a direct measure of the device's ability to convert solar energy into electricity [14]. The equation for calculating the PCE is given by:

$$PCE = \frac{J_{SC}\, V_{OC}\, FF}{P_{in}} \tag{10}$$

The open-circuit voltage V_{OC} is an indicator of the material quality in organic solar cells. It represents the maximum voltage a solar cell can generate in the absence of current flow in the external circuit, corresponding to the energy difference between the energy levels of electrons and holes in the photoactive material under illumination [95, 147–149]. A high V_{OC} value suggests that the solar cell has efficient charge transport

properties, resulting from an efficient alignment between the donor and acceptor energy levels. This alignment, due to a larger energy difference between the energy levels of electrons and holes, significantly reduces the probability of charge recombination, contributing to greater efficiency in charge transport and electric current generation [95, 150–152]. In a BHJ device, V_{OC} is determined by the energy difference between the HOMO of the donor and the LUMO of the acceptor, according to the largely used empirical Scharber equation [85, 153, 154]:

$$V_{oc} = \frac{1}{e}\left(\left|E^{D}_{HOMO} - E^{PCBM}_{LUMO}\right|\right) - 0.3\ V \tag{11}$$

where e represents the elementary charge, $E^{PCBM}_{LUMO} = -3.80\ eV$ [155] is the energy of the LUMO orbital of the typical acceptor material $PC_{61}BM$, and 0.3 V is an empirical correction accounting for transport losses to the electrodes [154]. For evaluating donor materials in DSSCs, the open-circuit voltage V_{oc} is calculated from the energy difference between the LUMO of the dye and the conduction band edge of the typical semiconductor TiO_2 in these systems as follows:

$$V_{oc} = \frac{1}{e}\left(\left|E^{Dye}_{LUMO} - E^{TiO_2}_{CB}\right|\right) \tag{12}$$

where $E^{TiO_2}_{CB}$ is the conduction band edge of TiO_2 equal to –4.0 eV [156]. Another important parameter for determining the PCE is the fill factor (FF), which can be approximated as a function of the open-circuit voltage V_{oc}, temperature T, and the Boltzmann constant k_B using the following expression:

$$FF = \frac{\frac{eV_{OC}}{k_B T} - \ln\left(\frac{eV_{OC}}{k_B T} + 0.72\right)}{\frac{eV_{OC}}{k_B T} + 1} \tag{13}$$

The short-circuit current, J_{SC}, in a solar cell is a significant parameter that reflects the device's ability to generate current under solar illumination [157, 158] It depends on factors such as light absorption by the donor material, the efficiency of electron-hole pair generation, charge collection efficiency, and the overlap between the material's absorption spectrum and the solar spectrum [159]. The greater this overlap and the more efficient the charge collection and transport processes, the higher the J_{SC} value. To compute J_{SC}, the external quantum efficiency (EQE) is integrated multiplied by the photon flux from the AM1.5 solar spectrum [160] over the relevant wavelength range [161]:

$$J_{SC} = e\int_{\lambda_{min}}^{\lambda_{max}} EQE(\lambda) \times photons(\lambda)d\lambda \quad (14)$$

This integration provides an accurate estimate of the generated current, offering a direct measure of the photocurrent performance of the solar cell and aiding in the optimization of materials and architectures to maximize device efficiency. In Eq. (14), λ_{min} and λ_{max} are the lower and upper wavelength limits of sunlight, respectively, under AM1.5 conditions. The AM1.5 spectrum is a standard reference for the spectral distribution of solar radiation. It refers to the global irradiance on a horizontal surface under a zenith angle of $\theta = 48.2°$, representing typical sunlight conditions when it reaches the Earth's surface, with a total irradiance of 1000 W.m^{-2} [149, 160]. EQE is defined as the step function Θ, equal to 0% for photon energies below the optical band gap E_{opt} of the donor material and to 65% for photon energies above this threshold,

$$EQE = 0.65 \times \Theta(\hbar\omega - E_{opt}) \quad (15)$$

where $\hbar\omega$ is the energy of the incident photon. In addition to the EQE, which assesses the proportion of photons converted into electric current, the light harvesting efficiency (LHE) quantifyes the material's ability to absorb incident photons:

$$LHE = 1 - 10^{-f} \quad (16)$$

where f represents the optical oscillator strength at the wavelength of maximum absorption λ_{max}. The LHE in DSSCs is directly related to J_{SC} because it represents the initial stage of light capture and absorption by the photosensitive dye, which is essential for generating electrical current in the device [76]. The LHE in DSSCs is related to J_{SC} through the following integral equation [76, 162],

$$J_{SC} = \int_{\lambda_{min}}^{\lambda_{max}} LHE(\lambda)\phi_{inject}\eta_{collect}d\lambda \quad (17)$$

where ϕ_{inject} is the electron injection efficiency and $\eta_{collect}$ represents the charge collection efficiency. $\eta_{collect}$ is considered constant and does not vary with the type of sensitizer used in the same DSSC device [76].

Driving Forces

In a solar cell, after light absorption by the active material, charge separation occurs at the donor-acceptor interface. The driving force for this dissociation is crucial to overcome the Coulombic attraction between the electron and hole in the exciton, thus allowing charges to be effectively separated [163–165]. The efficiency of this charge separation process is directly related to the solar cell's ability to generate electric current, as only dissociated free charges contribute to the current flow [166, 167]. Therefore, calculating the driving force for charge separation provides valuable insight into the device's efficiency potential, enabling the identification and enhancement of key parameters to maximize $PCEs$ and optimize the overall performance of the solar cell. One way to develop devices with high J_{SC} values is related to the driving force for charge separation in OSCs. This driving force plays a crucial role in overcoming the exciton binding energy, enabling the efficient dissociation of electron-hole pairs at the donor/acceptor interface. This process generates a larger number of free charges available for transport and collection at the electrodes, which directly contributes to an increase in J_{SC} [168]. In BHJ cells, the Gibbs free energy for the generation of separated charges,

which involves the transition from an initial singlet excited state, usually the S_1, with energy E_{opt}, to a final separated charge state with energy E_{CS}, is given by [164, 169]

$$\Delta G_{separation} = E_{opt} - E_{CS} \quad (18)$$

In this equation, E_{CS} is the energy difference between the LUMO of the acceptor and the HOMO of the donor, which we defined above as ΔE_{HL}^{D-A} in in Eq. (4) [164].

Eq. (14) for J_{SC} shows that another strategy to increase its values involves enhancing the electron injection efficiency ϕ_{inject}, which is directly related to the injection driving force (ΔG_{inject}). For DSSCs, the charge separation process can be evaluated by calculating the electron injection driving force, ΔG_{inject}, according to the equation [117, 170, 171]:

$$\Delta G_{inject} = E_{dye}^{*} - E_{CB}^{TiO_2} = (E_{dye} - E_{\lambda_{max}}) - E_{CB}^{TiO_2} \quad (19)$$

where $E_{CB}^{TiO_2}$ represents the value of the TiO_2 conduction band (-4.0 eV in vacuum), E_{dye}^{*} is the oxidation potential of the dye, which can be approximated by its respective E_{HOMO}, and $E_{\lambda_{max}}$ is the energy of the vertical transition associated with the maximum wavelength (λ_{max}).

Dye regeneration is a fundamental step in the operation of a DSSC, as it enables the replenishment of electrons transferred to the semiconductor, thereby maintaining the energy conversion cycle and ensuring device efficiency. Therefore, it is crucial to assess the effectiveness of this regeneration process through the regeneration driving force $\Delta G_{regenerate}$ defined as [76, 117, 170]

$$\Delta G_{regenerate} = E_{redox}^{I^-/I_3^-} - E_{dye} \quad (20)$$

where $E_{redox}^{I^-/I_3^-}$ represents the redox potential of the commonly used I^-/I_3^- electrolyte, with a value of -4.8 eV in vacuum. High values of both ΔG_{inject} and $\Delta G_{regenerate}$ enhance charge transfer efficiency between the semiconductor conduction band and the electrolyte, thus promoting effective electron injection and dye regeneration processes [76, 172].

In DSSCs, the dye is regenerated from its oxidized state within a few hundred picoseconds [173]. Thus, it is essential to compute the recombination driving force to evaluate the dye regeneration process. The free energy of the recombination rate can be determined by the following expression [76, 174]:

$$\Delta G_{recombination} = E_{CB}^{TiO_2} - E_{dye} = E_{CB}^{TiO_2} - E_{HOMO} \quad (21)$$

The optimal performance of a DSSC is often characterized by a low $\Delta G_{recombination}$ value, suggesting a controlled and less spontaneous electron recombination process, which is favorable for maintaining effective charge separation.

Reorganization energy

The reorganization energy (λ) in the framework of Marcus theory of electron transfer is a critical parameter for correlating efficiency and J_{SC} in photovoltaic devices such as BHJ solar cells and DSSCs [76, 175]. In these devices, λ represents the energetic cost associated with geometric relaxation during the charge transfer process and is inversely proportional to the mobility of charge carriers [176–178]. In DSSCs, λ is related to the process in which an electron is transferred from the dye to the semiconductor after photon absorption [76]. In contrast, in BHJ solar cells, the reorganization energy is associated with charge transfer at the donor-acceptor interface [176]. For the electron-donor materials used in the active layers of organic solar cells, higher hole mobility compared to electron mobility is particularly important, as it contributes to efficient charge transport and, consequently, to the optimized performance of the device [76].

The reorganization energy can be divided into two main components: internal reorganization (λ_{int}) and external reorganization (λ_{ext}) [178]. The internal component λ_{int}, usually the most significant, is related to structural changes and energy level shifts in the molecules involved in the charge transfer process. In contrast, λ_{ext} is associated with environmental variations, such as the polarization of the surrounding medium during the charge transfer process [178]. Since λ_{ext} is estimated to be significantly smaller than λ_{int}, its contribution is often considered negligible [176, 179]. Therefore, it is common to assume that $\lambda \approx \lambda_{int}$, which simplifies the analyses and calculations of the reorganization energy. The total reorganization energy can be calculated from equation (22), where λ_h is the reorganization energy for holes and λ_e is reorganization energy for electrons,

$$\lambda_{total} = \lambda_h + \lambda_e \tag{22}$$

where λ_h is obtained from the following equations:

$$\lambda_h = \lambda_h^{(1)} + \lambda_h^{(2)} \tag{22}$$

$$\lambda_h^{(1)} = E^{(1)}(M) - E^{(0)}(M) \tag{23}$$

$$\lambda_h^{(2)} = E^{(1)}(M^+) - E^{(0)}(M^+) \tag{24}$$

The terms in Eqs. (22) to (24) are defined in the diagram depicted in

Fig. 6. M and M^+ represent the neutral and positively charged species (containing the hole), respectively. $E^{(0)}(M)$ and $E^{(0)}(M^+)$ are the energies of the neutral and cationic states in their respective minimum-energy geometries. $E^{(1)}(M^+)$ and $E^{(1)}(M)$ correspond to the energy of the cationic state in the geometry of the neutral molecule and the energy of the neutral state in the geometry of the cationic molecule, respectively. ΔE is the adiabatic ionization energy, while $\lambda_h^{(1)}$and $\lambda_h^{(1)}$ are the geometric relaxation energies for the neutral and cationic states, respectively.

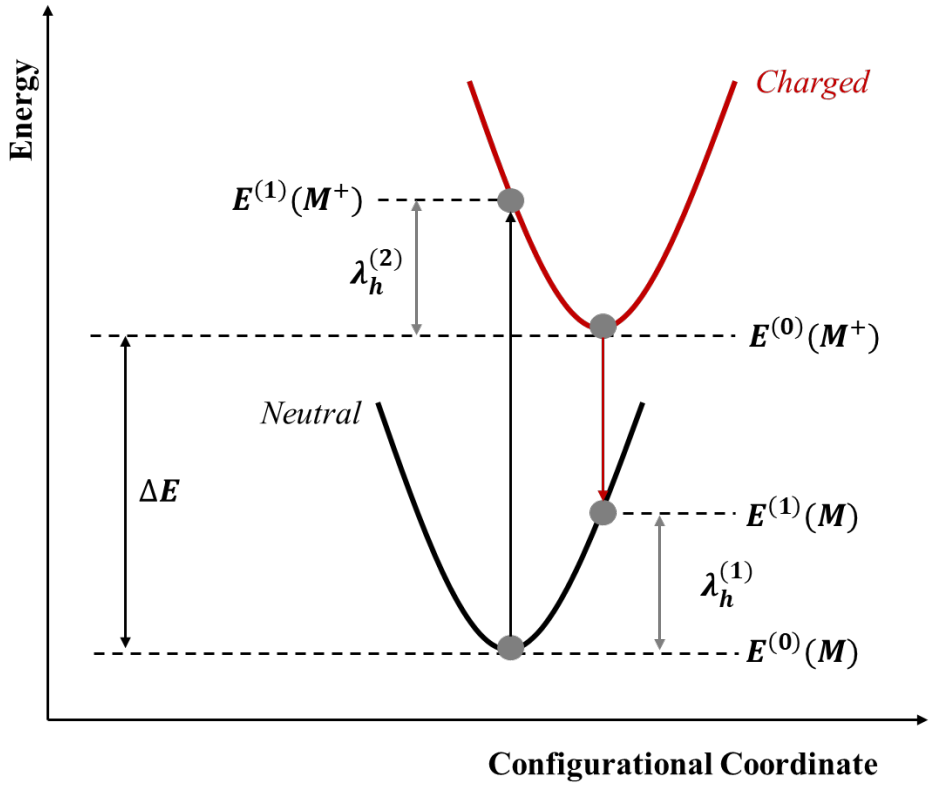

Fig. 6. Schematic representation of the potential energy surfaces for neutral and positively charged structures [176]. ΔE is the energy of adiabatic ionization, $E^{(0)}M$ and $E^{(0)}M^+$ are the energy of neutral and cationic states in the lower energy geometry, $E^{(1)}M$ and $E^{(1)}M^+$ the energy of cationic state in the geometry of the neutral molecule and the energy of neutral molecule in the geometry of the cationic molecule, and $\lambda_h^{(1)}$ and $\lambda_h^{(2)}$ are the energies of the geometric relaxation of the neutral and cationic states (reorganization energies), respectively.

The reorganization energy for electrons λ_e is obtained from similar equations:

$$\lambda_e = \lambda_e^{(1)} + \lambda_e^{(2)} \tag{25}$$

$$\lambda_e^{(1)} = E^{(1)}(M) - E^{(0)}(M) \tag{26}$$

$$\lambda_e^{(2)} = E^{(1)}(M^-) - E^{(0)}(M^-) \tag{27}$$

The hole transfer rate is inversely related to the reorganization energy involved in the process. Therefore, the higher the reorganization energy, the lower the hole mobility of the material. In general, reducing λ enhances charge transfer efficiency, allowing a larger proportion of photogenerated carriers to contribute to the photocurrent [76, 176]. For this reason, computing the reorganization energy is essential for optimizing the performance of devices such as BHJ and DSSC, providing insights for the development of materials that affords faster charge transport rates thus improved photovoltaic performance.

Global Reactivity Descriptors for Photovoltaics

Global reactivity descriptors are important quantities for understanding the electronic properties and predicting the reactive behavior of materials used in organic solar cells. These parameters enable the evaluation of stability and energy alignment between donor and acceptor components, which are critical factors for the efficiency of these devices. Ionization energy, electron affinity, chemical potential, hardness, and electronegativity values provide insights into charge transfer capabilities and exciton separation at the donor-acceptor interface. Electrophilicity values help identifying materials that can improve photoelectric efficiency. The analysis of these descriptors calculated using DFT can contribute to the rational design of new materials with optimized properties for high-performance photovoltaic devices.

Chemical hardness (η) is a parameter that reflects the stability of a compound and its resistance to electron exchange with the environment. Calculated by Eq. (28), chemical hardness is determined by the adiabatic ionization potential (IP) and the adiabatic electron affinity (EA), defined above. In general, the higher the chemical hardness of a compound, the greater its stability, indicating lower reactivity and higher resistance to electronic changes of its molecular state [180–182]. Chemical hardness is directly related to the conversion efficiency in DSSCs and BHJs because lower chemical hardness tends to result in higher conversion efficiency [183–186].

$$\eta = \frac{1}{2}(IP - EA) \tag{28}$$

Electrophilicity (ω), measures the tendency of a compound to accept electrons, and it is defined by Eq. (29). This index quantifies the energy stabilization of a system as it absorbs the maximum electron flow from a donor. Higher electrophilicity indicates a greater capacity for electron acceptance, reflecting the compound's reactivity in electron-transfer processes [185–187].

$$\omega = \frac{(IP + EA)^2}{4(IP - EA)} \tag{29}$$

A donor material for applications in a BHJ or DSSC is expected to exhibit a high electron-donating capacity along with a high electron-accepting capacity. The electron-donating power (ω^-) and electron-accepting power (ω^+) are useful parameters described by Eqs. (30) and (31) [188], which evaluate a molecule's ability to donate and accept electrons, respectively. A lower ω^- value indicates a higher electron-donating capacity, while a higher ω^+ value reflects a better ability to accept electrons [183, 186, 189].

$$\omega^+ = \frac{(IP + 3EA)^2}{16(IP - EA)} \tag{29}$$

$$\omega^- = \frac{(3IP + EA)^2}{16(IP - EA)} \tag{30}$$

Electronegativity (χ) [181, 190], defined as the ability of a compound to attract electrons, can be calculated by Eq. (31). In OSCs, compounds with high electronegativity values tend to attract electrons more strongly, which can increase charge recombination rates. This effect reduces the number of free charges for generating electrical current, negatively impacting the solar cell's efficiency. In dyes in DSSCs, an increase in dye

electronegativity is associated with a reduction in the open-circuit voltage (V_{OC}). The absolute electronegativity of the dye plays a crucial role in modulating electron diffusion, directly influencing the charge recombination mechanism through the dye [191].

$$\chi = \frac{(IP + EA)}{2} \tag{31}$$

Using Koopmann's theorem [192–194], these descriptors can be computed using HOMO and LUMO values. Koopmans' theorem establishes approximately the HOMO and LUMO energy values from the ionization potential (IP) and electron affinity (EA) in molecular systems according to the following expressions: $IP = -E_{HOMO}$ and $EA = -E_{LUMO}$. This implies that, in electronic structure calculations, the energies of the frontier orbitals can be directly used to estimate these properties. In a recent study [24], we showed that the using adiabatic IP and EA values provides an accurate description of electronic properties, as they account for the optimized geometries of ionic states, enabling a more realistic representation of electron loss and gain processes in the investigated systems.

In D-A-D systems based on diketopyrrolopyrrole (DPP) [24], global descriptors allowed the assessment of material stability, reactivity, and charge transfer capability, providing critical insights into HOMO-LUMO energy levels, charge separation efficiency, and potential applications in photovoltaic devices. Arunkumar and collaborators [73] investigated a series of D-π-A dyes based on tetrahydroquinoline, highlighting the relationship between chemical hardness and increased intramolecular charge transfer character. They identified two dyes with superior hole and electron transport properties, demonstrating their potential applicability in photovoltaic devices.

In summary, achieving high efficiency in DSSCs and BHJs OSCs requires optimizing several fundamental parameters related to charge separation, electron injection, dye regeneration, and reduction of charge recombination rates. When considered together, these theoretical evaluations provide a comprehensive understanding

of the factors influencing efficiency in these OSCs, providing a solid foundation for targeted improvements in material design and device architecture. By focusing on these properties, researchers can adjust the balance of internal processes within OSCs more precisely, promoting significant advancements in performance and long-term stability for next-generation photovoltaic devices.

The importance of a judicious choice of the exchange-correlation functional in DFT for obtaining accurate values of HOMO and LUMO for computing optoelectronic properties

Selecting the appropriate exchange-correlation functional and basis set directly impacts the accuracy of the frontier orbital values, used to compute the optoelectronic properties of organic materials for OPVs according to the formulae above.

Hybrid functionals such as B3LYP [195] are widely used in organic systems due to their good balance between accuracy and computational cost, providing reliable results for general electronic properties [25, 196–201]. However, the selection of hybrid functionals should be approached with caution, as they may underestimate the spatial separation between frontier orbitals and may describe poorly charge transfer effects [202–206]. Overall, E_{HOMO} values predicted by hybrid functionals are more accurate than those obtained with pure functionals, which depend exclusively on the local or semi-local electron densities and are relatively sensitive to the fraction of Hartree-Fock (HF) exchange [204, 207]. Functionals with higher HF exchange fractions usually yield more accurate E_{HOMO} values, which are particularly relevant for systems where orbital localization and charge separation are critical for photovoltaic performance [204, 208].

Although higher HF exchange fractions improve the accuracy of HOMO levels, they frequently overestimate LUMO energies and, consequently, widen the HOMO-LUMO gap. Moreover, as highlighted by Zhang and collaborators [204], generalized gradient approximation (GGA) functionals have a smaller systematic error in predicting HOMO-LUMO gaps, despite inaccuracies in the absolute values of orbital levels.

Including a significant fraction of HF exchange in long-range functionals, such as in CAM-B3LYP, further degrades the accuracy of E_{LUMO} values, leading to predictions that can significantly diverge from experimental data [204, 208, 209].

Khan and collaborators recently studied seven donor molecules based on benzo[1,2-b:4,5-b′]dithiophene (BDT) with an A-π-D-π-A configuration, using DFT and time dependent (TD)-DFT methods. The analysis of maximum absorption wavelengths identified the CAM-B3LYP functional as the most accurate, outperforming ωB97XD, B3LYP, and MPW1PW91 [70]. In a similar study, Bora and collaborators designed five new donor-π-acceptor-π-donor (D–π–A–π–D)-type conjugated acceptors, employing quinacridone as the donor, thiophene as the π bridge component, and five distinct central acceptor units. By correlating the calculated HOMO and LUMO energies, the gap energy E_g, and absorption wavelength values (λ_{max}) with experimental data, they found that the HSEH1PBE functional, using the 6-31G(d) basis set, showed the best agreement with experimental results compared to B3LYP, B3PW91, B3LYP-D3, CAM-B3LYP, PBEPBE, and ωB97XD [210].

We recently investigated the design and application in BHJ and DSSC OSCs of nine star-shaped molecules with a triazine (Tr) core built with thiophene (Th), phenyl (Ph), and carbazole (Cz) fragments. For the Tr-Th and Tr-Cz systems, we used TD-DFT to calculate excited-state electronics properties, using the B3LYP, PBE, M06-2X, CAM-B3LYP, ωB97XD, and LC-wPBE functionals. We found that the B3LYP frontier molecular orbital energy values agreed with available experimental data and similar systems containing the triazine core. Although the PBE functional also yielded good results, with deviations of approximately 11% for HOMO and LUMO energy values in the Tr-Cz system, B3LYP provided a more balanced combination of accuracy and computational cost. Despite the low fraction of HF exchange, which is relevant for systems having significant charge transfer effects, as in semiconductor polymers, the B3LYP functional remains widely used, with a large body of recent studies showing satisfactory results for calculating optoelectronic properties in donor and acceptor materials for organic photovoltaic devices [211, 212]. Many investigations have shown that, although B3LYP may underestimate some electronic properties of conjugated

organic systems, it still offers good relative accuracy in predicting HOMO and LUMO energy levels and optical gaps. Its simplicity, along with a good balance between computational cost and accuracy, makes B3LYP a popular choice in research focused on designing and optimizing materials for OSCs [25, 211–216].

Finally, it is important to highlight the recommendations of Bursch and collaborators [203], which guide the selection of the functional based on the chemical system and the specific task, rather than on popularity alone. First, it is advisable always to include a dispersion correction to improve accuracy in intermolecular interactions. Additionally, it is recommended to assess cost-effective combinations, considering the use of (m)GGA-type functionals, which, although less precise than hybrids, offer lower computational costs. Hybrid functionals are preferred for accuracy, but their use should be balanced against computational demand. Verifying consistency across different classes of functionals—such as comparing a hybrid with an (m)GGA—is also suggested, especially in comparative analyses. In critical cases, it may be useful to test hybrids that include different fractions of HF exchange to ensure that the results accurately reflect the properties of the system under study.

The choice of basis set is a crucial factor for the accuracy of optoelectronic property calculations and should consider the type of system studied, the required precision, and computational cost. Basis sets such as 6-31G(d,p) [200, 217, 218] or 6-311G(d,p)[212, 216, 219, 220] are widely used for medium-sized organic molecules, as they balance cost and accuracy, making them suitable for fundamental electronic properties like HOMO-LUMO energy levels. For systems requiring higher accuracy, especially in large conjugated structures, basis sets like Def2-SVP [25, 221–223] or Def2-TZVP[223–225] are recommended due to their detailed descriptions of electronic interactions and orbitals. Thus, the selection should balance available computational resources with the level of detail required by the study.

On the importance of the DFT HOMO and LUMO value for computing the OPV properties: the triazine molecule as an illustrative case

The relationship between PCE in OSCs and HOMO-LUMO energy levels is directly associated with fundamental processes such as charge separation, electron, and hole transport, and charge recombination. The alignment between donor and acceptor HOMO and LUMO energy levels, for instance, plays a crucial role in determining the open-circuit voltage (V_{OC}), a key parameter for achieving good PCE values.

We recently investigated [25] the influence of the choice of functional on the determination of the HOMO and LUMO energy levels in donor-acceptor (D-A) systems with a triazine (Tr) nucleus. We investigated nine star molecules with this nucleus, having found PCE values close to 30% due to a favorable alignment of the energy levels. The calculations employed the B3LYP, PBE, M06-2X, CAM-B3LYP, wB97XD, and LC-wPBE functionals, to analyze their impact on the optoelectronic properties of the systems.

The literature indicates that, for conjugated D-A systems containing a triazine nucleus, the HOMO and LUMO energy values typically vary between -5.0 and -6.0 eV (HOMO) and between -1.5 and -3.5 eV () [226,227,228,229]. In our work, we found that the B3LYP functional produced the smallest deviations compared to the experimental data, with only 0.6% deviation for the HOMO and 37.4% for the LUMO. The PBE functional also presented good results, with deviations close to 11%, but the B3LYP stood out for providing a more balanced combination between accuracy and computational cost.

The analysis of the HOMO and LUMO levels showed a significant influence on the optoelectronic properties of the systems, in particular on the band gap energy (E_g). The wB97XD E_g values were significantly higher, around 7.6 eV, in contrast to the B3LYP results, around 3.9 eV. Although the corresponding exciton binding energy (E_{bind}) did not show substantial variations between the two functionals, the parameters related to the driving force showed a significant dependence on the HOMO and LUMO energy levels.

In addition, parameters such as V_{OC} and PCE were also shown to be strongly influenced by the frontier orbitals. For the systems containing a triazine core, the wB97XD functional resulted in a maximum PCE value of 10.58% for a BHJ and 10.26% for a DSSC. On the other hand, the B3LYP functional led to a maximum PCE of 32.39%, evidencing that the precision in the alignment of the HOMO and LUMO levels can drastically affect the optoelectronic properties of OPVs.

Systems with optimized HOMO-LUMO levels favored charge transport by reducing recombination rates and improving electron and hole mobility. In triazine-based systems, substituents such as carbazole stabilized these energy levels, positively impacting photovoltaic performance. These results emphasize the importance of adjusting computational methods and molecular design to optimize energy level alignment and improve the efficiency of photovoltaic devices.

Conclusion

This work systematically presented the main processes involved in producing an electric current in BHJ solar cells and DSSCs. We discussed these processes in detail and presented several simple equations for computing relevant practical properties of these devices using DFT. We also discussed the limitations of this approach, mainly related to the choice of the exchange-correlation functional.

By providing reliable and accurate predictions, DFT-based methods can accelerate the screening of promising materials, significantly reducing the time and costs associated with laboratory experiments. Furthermore, DFT can facilitate the rational design of donor and acceptor materials, allowing for precise tuning of their electronic and structural properties to maximize performance. This approach has been essential in addressing challenges such as exciton dissociation, charge recombination, and device stability, leading to significant advancements in the field. Although significant advances have been made in understanding the relationship between electronic properties and the efficiency of organic photovoltaic devices, challenges remain, including the need for a comprehensive evaluation of functionals and basis sets suitable for different chemical systems. In this context, we emphasize the importance of selecting computational

methodologies appropriate to the specific problem, striving to balance computational cost and accuracy.

References

1. Smets AHM, Jäger Klaus, Isabella Olindo, et al (2016) Solar energy: the physics and engineering of photovoltaic conversion, technologies and systems. UIT Cambridge Ltd., Cambridge

2. Herzog A V, Lipman TE, Kammen DM Renewable Energy Sources. In: Perspectives and Overview of Life Support Systems and Sustainable Development. https://www.eolss.net/sample-chapters/c08/E3-03-27.pdf Accessed 15 Dec 2024

3. Energy Institute (2024) Statistical Review of World Energy. https://www.energyinst.org/statistical-review Accessed 15 Dec 2024

4. Ferruzzi G, Delcea C, Barberi A, et al (2023) Concentrating Solar Power: The State of the Art, Research Gaps and Future Perspectives. Energies (Basel) 16:1–39. https://doi.org/10.3390/en16248082

5. Pazheri FR, Othman MF, Malik NH (2014) A review on global renewable electricity scenario. Renewable and Sustainable Energy Reviews 31:835–845. https://doi.org/10.1016/j.rser.2013.12.020

6. Lyu X, Ruan T, Wang W, Cai X (2024) A bibliometric evaluation and visualization of global solar power generation research: productivity, contributors and hot topics. Environmental Science and Pollution Research 31:8274–8290. https://doi.org/10.1007/s11356-023-31715-x

7. Thirugnanasambandam M, Iniyan S, Goic R (2010) A review of solar thermal technologies. Renewable and Sustainable Energy Reviews 14:312–322. https://doi.org/10.1016/j.rser.2009.07.014

8. Subtil Lacerda J, Van Den Bergh JCJM (2016) Diversity in solar photovoltaic energy: Implications for innovation and policy. Renewable and Sustainable Energy Reviews 54:331–340. https://doi.org/10.1016/j.rser.2015.10.032

9. Sampaio PGV, González MOA (2017) Photovoltaic solar energy: Conceptual framework. Renewable and Sustainable Energy Reviews 74:590–601. https://doi.org/10.1016/j.rser.2017.02.081

10. Green MA (2000) Photovoltaics: technology overview. Energy Policy 28:989–998. https://doi.org/10.1063/1.1697243

11. Sano M, Pope M, Kallmann H (1965) Electroluminescence and band gap in anthracene. J Chem Phys 43:2920–2921. https://doi.org/10.1063/1.1697243

12. Pope M, Kallmann HP, Magnante P (1963) Electroluminescence in organic crystals. J Chem Phys 38:2042–2043. https://doi.org/10.1063/1.1733929

13. Helfrich W, Schneider WG (1965) Recombination Radiation in Anthracene Crystals. Phys Rev Lett 14:229–231. https://doi.org/10.1103/PhysRevLett.14.229

14. Ostroverkhova O (2016) Organic Optoelectronic Materials: Mechanisms and Applications. Chem Rev 116:13279–13412. https://doi.org/10.1021/acs.chemrev.6b00127

15. Köhler A, Bässler H (2015) Electronic Processes in Organic Semiconductors, First Edition. Wiley-VCH, Weinheim, Germany

16. Douglass Plenum DH, York N, M Varma by C, et al (1959) Electrical Conductivity in Doped Polyacetylene. Phys Rev Lett 39:415. https://doi.org/10.1103/PhysRevLett.39.1098

17. Chiang CK, Park YW, Heeger AJ, et al (1978) Conducting polymers: Halogen doped polyacetylene. J Chem Phys 69:5098–5104. https://doi.org/10.1063/1.436503

18. Hideki Shirakawa B, Louis EJ, Macdiarmid AG, et al (1977) Synthesis of Electrically Conducting Organic Polymers : Halogen Derivatives of Polyacetylene, (CH)x. J Chem Soc Chem Commun 578–580. https://doi.org/10.1039/C39770000578

19. Borges I, Aquino AJA, Köhn A, et al (2013) Ab initio modeling of excitonic and Charge-transfer states in organic semiconductors: The PTB1/PCBM low band gap system. J Am Chem Soc 135:18252–18255. https://doi.org/10.1021/ja4081925

20. Gupta N, Nagar MR, Anamika, et al (2022) Triazine and Thiophene-Containing Conjugated Polymer Network Emitter-Based Solution-Processable Stable Blue Organic LEDs. ACS Appl Polym Mater 5:130–140. https://doi.org/10.1021/acsapm.2c01337

21. Rasool A, Zahid S, Ans M, et al (2022) Bithieno Thiophene-Based Small Molecules for Application as Donor Materials for Organic Solar Cells and Hole Transport Materials for Perovskite Solar Cells. ACS Omega 7:844–862. https://doi.org/10.1021/acsomega.1c05504

22. Zhou H, Yang L, You W (2012) Rational design of high performance conjugated polymers for organic solar cells. Macromolecules 45:607–632. https://doi.org/10.1021/ma201648t

23. Sun D, Si C, Wang T, Zysman-Colman E (2022) 1,3,5-Triazine-Functionalized Thermally Activated Delayed Fluorescence Emitters for Organic Light-Emitting Diodes. Adv Photonics Res 3:1-54. https://doi.org/10.1002/adpr.202200203

24. Rosa NMP, Borges I (2024) Photophysical properties of donor (D)–acceptor (A)–donor (D) diketopyrrolopyrrole (A) systems as donors for applications to organic electronic devices. J Comput Chem 45:2885–2898. https://doi.org/10.1002/jcc.27492

25. Rosa NMP, Borges I (2024) Star-Shaped Molecules with a Triazine Core: (TD)DFT Investigation of Charge Transfer and Photovoltaic Properties of Organic Solar Cells. Brazilian Journal of Physics 54:252. https://doi.org/10.1007/s13538-024-01636-2

26. Kaur N, Singh M, Pathak D, et al (2014) Organic materials for photovoltaic applications: Review and mechanism. Synth Met 190:20–26. https://doi.org/10.1016/j.synthmet.2014.01.022

27. Oni AM, Mohsin ASM, Rahman MM, Hossain Bhuian MB (2024) A comprehensive evaluation of solar cell technologies, associated loss mechanisms, and efficiency enhancement strategies for photovoltaic cells. Energy Reports 11:3345–3366. https://doi.org/10.1016/j.egyr.2024.03.007

28. Zhu L, Zhang M, Xu J, et al (2022) Single-junction organic solar cells with over 19% efficiency enabled by a refined double-fibril network morphology. Nat Mater 21:656–663. https://doi.org/10.1038/s41563-022-01244-y

29. Wang J, Zheng Z, Zu Y, et al (2021) A Tandem Organic Photovoltaic Cell with 19.6% Efficiency Enabled by Light Distribution Control. Advanced Materials 33:1-9. https://doi.org/10.1002/adma.202102787

30. Chong K, Xu X, Meng H, et al (2022) Realizing 19.05% Efficiency Polymer Solar Cells by Progressively Improving Charge Extraction and Suppressing Charge Recombination. Advanced Materials 34:1-11. https://doi.org/10.1002/adma.202109516

31. Zhang KN, Du XY, Yan L, et al (2024) Organic Photovoltaic Stability: Understanding the Role of Engineering Exciton and Charge Carrier Dynamics from Recent Progress. Small Methods 8:1-29. https://doi.org/10.1002/smtd.202300397

32. Li C, Zhou J, Song J, et al (2021) Non-fullerene acceptors with branched side chains and improved molecular packing to exceed 18% efficiency in organic solar cells. Nat Energy 6:605–613. https://doi.org/10.1038/s41560-021-00820-x

33. Cui Y, Xu Y, Yao H, et al (2021) Single-Junction Organic Photovoltaic Cell with 19% Efficiency. Advanced Materials 33:1-8. https://doi.org/10.1002/adma.202102420

34. Zheng Z, Wang J, Bi P, et al (2022) Tandem Organic Solar Cell with 20.2% Efficiency. Joule 6:171–184. https://doi.org/10.1016/j.joule.2021.12.017

35. Cusumano P, Arnone C, Giambra MA, Parisi A (2020) Donor/acceptor heterojunction organic solar cells. Electronics (Switzerland) 9:1-8. https://doi.org/10.3390/electronics9010070

36. Malk FH, Abdul Karem AAH, Al – Tememe EH (2022) Organic Solar Cells: Short Review. MINAR International Journal of Applied Sciences and Technology 4:174–181. https://doi.org/10.47832/2717-8234.13.16

37. Clarke TM, Durrant JR (2010) Charge photogeneration in organic solar cells. Chem Rev 110:6736–6767. https://doi.org/10.1021/cr900271s

38. Balzer D, Kassal I (2024) Delocalisation enables efficient charge generation in organic photovoltaics, even with little to no energetic offset. Chem Sci. 15:4779-4789. https://doi.org/10.1039/d3sc05409h

39. Firdaus Y, Le Corre VM, Karuthedath S, et al (2020) Long-range exciton diffusion in molecular non-fullerene acceptors. Nat Commun 11:1-10. https://doi.org/10.1038/s41467-020-19029-9

40. Solak EK, Irmak E (2023) Advances in organic photovoltaic cells: a comprehensive review of materials, technologies, and performance. RSC Adv 13:12244–12269. https://doi.org/10.1039/d3ra01454a

41. Schlenker CW, Thompson ME (2012) Current challenges in organic photovoltaic solar energy conversion. Top Curr Chem 312:175–212. https://doi.org/10.1007/128_2011_219

42. Reese MO, Nardes AM, Rupert BL, et al (2010) Photoinduced degradation of polymer and polymer-fullerene active layers: Experiment and theory. Adv Funct Mater 20:3476–3483. https://doi.org/10.1002/adfm.201001079

43. Rafique S, Abdullah SM, Sulaiman K, Iwamoto M (2018) Fundamentals of bulk heterojunction organic solar cells: An overview of stability/degradation issues and strategies for improvement. Renewable and Sustainable Energy Reviews 84:43–53. https://doi.org/10.1016/j.rser.2017.12.008

44. Liu Q, Jiang Y, Jin K, et al (2020) 18% Efficiency organic solar cells. Sci Bull (Beijing) 65:272–275. https://doi.org/10.1016/j.scib.2020.01.001

45. Jing J, Dong S, Zhang K, et al (2022) Semitransparent Organic Solar Cells with Efficiency Surpassing 15%. Adv Energy Mater 12:1-11. https://doi.org/10.1002/aenm.202200453

46. Cui Y, Xu Y, Yao H, et al (2021) Single-Junction Organic Photovoltaic Cell with 19% Efficiency. Advanced Materials 33:1-8. https://doi.org/10.1002/adma.202102420

47. Green MA, Dunlop ED, Hohl-Ebinger J, et al (2020) Solar cell efficiency tables (Version 55). Progress in Photovoltaics: Research and Applications 28:3–15. https://doi.org/10.1002/pip.3228

48. Green MA, Dunlop ED, Yoshita M, et al (2024) Solar cell efficiency tables (Version 64). Progress in Photovoltaics: Research and Applications 32:425–441. https://doi.org/10.1002/pip.3831

49. Green M, Dunlop E, Hohl-Ebinger J, et al (2021) Solar cell efficiency tables (version 57). Progress in Photovoltaics: Research and Applications 29:3–15. https://doi.org/10.1002/pip.3371

50. Green MA, Emery K, Hishikawa Y, et al (2015) Solar cell efficiency tables (Version 45). Progress in Photovoltaics: Research and Applications 23:1–9. https://doi.org/10.1002/pip.2573

51. Green MA, Emery K, Hishikawa Y, et al (2017) Solar cell efficiency tables (version 49). Progress in Photovoltaics: Research and Applications 25:3–13. https://doi.org/10.1002/pip.2855

52. Green MA, Hishikawa Y, Dunlop ED, et al (2018) Solar cell efficiency tables (version 51). Progress in Photovoltaics: Research and Applications 26:3–12. https://doi.org/10.1002/pip.297

53. Green MA, Dunlop ED, Hohl-Ebinger J, et al (2022) Solar cell efficiency tables (version 59). Progress in Photovoltaics: Research and Applications 30:3–12. https://doi.org/10.1002/pip.3506

54. Green MA, Hishikawa Y, Dunlop ED, et al (2019) Solar cell efficiency tables (Version 53). Progress in Photovoltaics: Research and Applications 27:3–12. https://doi.org/10.1002/pip.3102

55. Green MA, Dunlop ED, Yoshita M, et al (2024) Solar cell efficiency tables (Version 63). Progress in Photovoltaics: Research and Applications 32:3–13. https://doi.org/10.1002/pip.3750

56. Green MA, Dunlop ED, Siefer G, et al (2023) Solar cell efficiency tables (Version 61). Progress in Photovoltaics: Research and Applications 31:3–16. https://doi.org/10.1002/pip.3646

57. Green MA, Emery K, Hishikawa Y, et al (2013) Solar cell efficiency tables (version 41). Progress in Photovoltaics: Research and Applications 21:1–11. https://doi.org/10.1002/pip.2352

58. Green MA, Emery K, Hishikawa Y, et al (2014) Solar cell efficiency tables (version 43). Progress in Photovoltaics: Research and Applications 22:1–9. https://doi.org/10.1002/pip.2452

59. Green MA, Emery K, Hishikawa Y, Warta W (2011) Solar cell efficiency tables (version 37). Progress in Photovoltaics: Research and Applications 19:84–92. https://doi.org/10.1002/pip.1088

60. Green MA, Emery K, Hishikawa Y, et al (2016) Solar cell efficiency tables (version 47). Progress in Photovoltaics: Research and Applications 24:3–11. https://doi.org/10.1002/pip.2728

61. Green MA, Emery K, Hishikawa Y, et al (2012) Solar cell efficiency tables (version 39). Progress in Photovoltaics: Research and Applications 20:12–20. https://doi.org/10.1002/pip.2163

62. Green MA, Emery K, Hishikawa Y, Warta W (2010) Solar cell efficiency tables (version 35). Progress in Photovoltaics: Research and Applications 18:144–150. https://doi.org/10.1002/pip.974

63. Green MA, Emery K, Hishikawa Y, Warta W (2009) Solar cell efficiency tables (Version 33). Progress in Photovoltaics: Research and Applications 17:85–94. https://doi.org/10.1002/pip.880

64. Green MA, Emery K, King DL, et al (2007) Solar cell efficiency tables (version 29). Progress in Photovoltaics: Research and Applications 15:35–40. https://doi.org/10.1002/pip.741

65. Green MA, Emery K, Hishikawa Y, Warta W (2008) Solar cell efficiency tables (version 31). Progress in Photovoltaics: Research and Applications 16:61–67. https://doi.org/10.1002/pip.808

66. Hösel M, Søndergaard RR, Jørgensen M, Krebs FC (2014) Failure modes and fast repair procedures in high voltage organic solar cell installations. Adv Energy Mater 4:1-7. https://doi.org/10.1002/aenm.201301625

67. Modesto-Costa L, Borges I, Aquino AJA, Lischka H (2018) Electronic structure theory gives insights into the higher efficiency of the PTB electron-donor

polymers for organic photovoltaics in comparison with prototypical P3HT. Journal of Chemical Physics 149:1–7. https://doi.org/10.1063/1.5054919

68. Borges I, Uhl E, Modesto-Costa L, et al (2016) Insight into the Excited State Electronic and Structural Properties of the Organic Photovoltaic Donor Polymer Poly(thieno[3,4-b]thiophene benzodithiophene) by Means of ab Initio and Density Functional Theory. Journal of Physical Chemistry C 120:21818–21826. https://doi.org/10.1021/acs.jpcc.6b07689

69. Sharma SJ, Sekar N (2024) Exploring charge transfer effects on linear, non-linear optical, and dye-sensitized solar cell properties: A DFT and TD-DFT investigation of carbazole and aniline-based dyes. Int J Quantum Chem 124:1-22. https://doi.org/10.1002/qua.27419

70. Usman Khan M, Shafiq F, Ramzan Saeed Ashraf Janjua M, et al (2024) Predicting benzodithiophene based donor materials with enhanced 19.09% PCE, open-circuit voltage and optoelectronic attributes for solar cell applications: Photochemical insights from DFT. J Photochem Photobiol A Chem 446:1-16. https://doi.org/10.1016/j.jphotochem.2023.115115

71. Pourebrahimi S, Pirooz M (2024) Exploring the optoelectronic properties of Flavylium cations as acceptors in organic solar Cells: DFT/TD-DFT investigations. Solar Energy 275:1–11. https://doi.org/10.1016/j.solener.2024.112617

72. Mejbel HK, Al-Badry LF (2024) Tuning the optoelectronic properties for small organic compounds as organic solar cell applications. Optoelectron Lett 20:412–417. https://doi.org/10.1007/s11801-024-3165-7

73. Arunkumar A, Ju XH (2024) Computational method on highly efficient D-π-A-π-D-based different molecular acceptors for organic solar cells applications and non-linear optical behaviour. Spectrochim Acta A Mol Biomol Spectrosc 317:1-15. https://doi.org/10.1016/j.saa.2024.124391

74. Sadiq S, Khera RA, Tawfeek AM, et al (2024) Theoretical investigation of substituted end groups in thiophene-phenyl-thiophene (TPT) derivatives for high efficiency organic solar cells. J Phys Org Chem 37:1-15. https://doi.org/10.1002/poc.4607

75. Le Bahers T, Labat F, Pauporté T, et al (2011) Theoretical procedure for optimizing dye-sensitized solar cells: From electronic structure to photovoltaic efficiency. J Am Chem Soc 133:8005–8013. https://doi.org/10.1021/ja201944g

76. Conradie J (2024) Effective dyes for DSSCs–Important experimental and calculated parameters. Energy Nexus 13:1-15. https://doi.org/10.1016/j.nexus.2024.100282

77. Bernède JC (2008) Organic Photovoltaic Cells: History, Principle and Techniques. J Chil Chem Soc 53:1549-1564. https://doi.org/10.4067/S0717-97072008000300001

78. Moliton A, Nunzi JM (2006) How to model the behaviour of organic photovoltaic cells. Polym Int 55:583–600. https://doi.org/10.1002/pi.2038

79. Ramoroka ME, Yussuf ST, Nwambaekwe KC, et al (2024) Advances in Organic Photovoltaic Cells: Fine-Tuning of the Photovoltaic Processes. Solar RRL 8:1-29. https://doi.org/10.1002/solr.202300982

80. Nelson J (2002) Organic photovoltaic films. Curr Opin Solid State Mater Sci 6:87–95. https://doi.org/10.1016/S1359-0286(02)00006-2

81. Sampaio PGV, González MOA (2022) A review on organic photovoltaic cell. Int J Energy Res 46:17813–17828 https://doi.org/10.1002/er.8456

82. Borges I, Guimarães RMPO, Monteiro-de-Castro G, et al (2023) A comprehensive analysis of charge transfer effects on donor-pyrene (bridge)-acceptor systems using different substituents. J Comput Chem 44:2424–2436. https://doi.org/10.1002/jcc.27208

83. Liu H, Geng Y, Xiao Z, et al (2024) The Development of Quinoxaline-Based Electron Acceptors for High Performance Organic Solar Cells. Advanced Materials. 36:1-35. https://doi.org/10.1002/adma.202404660

84. Zhou D, Wang Y, Yang S, et al (2024) Recent Advances of Benzodithiophene-Based Donor Materials for Organic Solar Cells. Small. 20:1-67. https://doi.org/10.1002/smll.202306854

85. Scharber MC, Sariciftci NS (2013) Efficiency of bulk-heterojunction organic solar cells. Prog Polym Sci 38:1929–1940. https://doi.org/10.1016/j.progpolymsci.2013.05.001

86. Grätzel M (2003) Dye-sensitized solar cells. Journal of Photochemistry and Photobiology C: Photochemistry Reviews 4:145–153. https://doi.org/10.1016/S1389-5567(03)00026-1

87. Hagfeldt A, Boschloo G, Sun L, et al (2010) Dye-sensitized solar cells. Chem Rev 110:6595–6663. https://doi.org/10.1021/cr900356p

88. Jean R (2009) Molecular bulk heterojunctions: An emerging approach to organic solar cells. Acc Chem Res 42:1719–1730. https://doi.org/10.1021/ar900041b

89. Lu L, Zheng T, Wu Q, et al (2015) Recent Advances in Bulk Heterojunction Polymer Solar Cells. Chem Rev 115:12666–12731. https://doi.org/10.1021/acs.chemrev.5b00098

90. Deibel C, Dyakonov V (2010) Polymer-fullerene bulk heterojunction solar cells. Reports on Progress in Physics 73:1-40. https://doi.org/10.1088/0034-4885/73/9/096401

91. Facchetti A (2013) Polymer donor-polymer acceptor (all-polymer) solar cells. Materials Today 16:123–132. https://doi.org/10.1016/j.mattod.2013.04.005

92. Dou L, You J, Hong Z, et al (2013) 25th anniversary article: A decade of organic/polymeric photovoltaic research. Advanced Materials 25:6642–6671. https://doi.org/10.1002/adma.201302563

93. Meftah M, Damé L, Bolsée D, et al (2018) SOLAR-ISS: A new reference spectrum based on SOLAR/SOLSPEC observations. Astron Astrophys 611:1-14. https://doi.org/10.1051/0004-6361/201731316

94. Mayer AC, Scully SR, Hardin BE, et al (2007) Polymer-based solar cells. https://doi.org/10.1016/S1369-7021(07)70276-6

95. Qi B, Wang J (2012) Open-circuit voltage in organic solar cells. J Mater Chem 22:24315–24325. https://doi.org/10.1039/c2jm33719c

96. Cui C, Li Y (2019) High-performance conjugated polymer donor materials for polymer solar cells with narrow-bandgap nonfullerene acceptors. Energy Environ Sci 12:3225–3246 https://doi.org/10.1039/C9EE02531F

97. Yang H, Cui C, Li Y (2021) Effects of Heteroatom Substitution on the Photovoltaic Performance of Donor Materials in Organic Solar Cells. Acc Mater Res 2:986–997. https://doi.org/10.1021/accountsmr.1c00119

98. He K, Kumar P, Yuan Y, et al (2021) A Wide Bandgap Polymer Donor Composed of Benzodithiophene and Oxime-Substituted Thiophene for High-Performance Organic Solar Cells. ACS Appl Mater Interfaces 13:26441–26450. https://doi.org/10.1021/acsami.1c02442

99. An C, Zheng Z, Hou J (2020) Recent progress in wide bandgap conjugated polymer donors for high-performance nonfullerene organic photovoltaics. Chemical Communications 56:4750–4760. https://doi.org/10.1039/d0cc01038c

100. Fakharuddin A, Jose R, Brown TM, et al (2014) A perspective on the production of dye-sensitized solar modules. Energy Environ Sci 7:3952–3981. https://doi.org/10.1039/C4EE01724B

101. Ashok A, Mathew SE, Shivaram SB, et al (2018) Cost effective natural photo-sensitizer from upcycled jackfruit rags for dye sensitized solar cells. Journal of Science: Advanced Materials and Devices 3:213–220. https://doi.org/10.1016/j.jsamd.2018.04.006

102. Avilés-Betanzos R, Oskam G, Pourjafari D (2023) Low-Temperature Fabrication of Flexible Dye-Sensitized Solar Cells: Influence of Electrolyte Solution on Performance under Solar and Indoor Illumination. Energies (Basel) 16:1–35. https://doi.org/10.3390/en16155617

103. Li G, Sheng L, Li T, et al (2019) Engineering flexible dye-sensitized solar cells for portable electronics. Solar Energy 177:80–98. https://doi.org/10.1016/j.solener.2018.11.017

104. Hendi AA, Alanazi MM, Alharbi W, et al (2023) Dye-sensitized solar cells constructed using titanium oxide nanoparticles and green dyes as photosensitizers. J King Saud Univ Sci 35:1–7. https://doi.org/10.1016/j.jksus.2023.102555

105. Alessa H, Wijayantha KGU (2024) A very simple flexible tandem dye-sensitized solar cell. Journal of Umm Al-Qura University for Applied Sciences 1–9. https://doi.org/10.1007/s43994-024-00136-y

106. Shakeel Ahmad M, Pandey AK, Abd Rahim N (2017) Advancements in the development of TiO2 photoanodes and its fabrication methods for dye sensitized solar cell (DSSC) applications. A review. Renewable and Sustainable Energy Reviews 77:89–108. https://doi.org/10.1016/j.rser.2017.03.129

107. Jamalullail N, Mohamad IS, Norizan MN, et al (2017) Recent improvements on TiO2 and ZnO nanostructure photoanode for dye sensitized solar cells: A brief review. EPJ Web Conf 162:1–5. https://doi.org/10.1051/epjconf/201716201045

108. Kannan S (2018) A Review on Titanium Dioxide For Dye Sensitized Solar Cells Application. Int J Curr Adv Res 7:10575–10579. https://doi.org/10.24327/ijcar.2018.10579.1797

109. Shaban S, Pradhan S, Pandey SS (2023) Fabrication and Characterization of Bifacial Dye-Sensitized Solar Cells Utilizing Indoline Dye with Iodine- and Cobalt-Based Redox Electrolytes. Physica Status Solidi (A) Applications and Materials Science 220:1–7. https://doi.org/10.1002/pssa.202300241

110. Jeon J, Park YC, Han SS, et al (2014) Rapid dye regeneration mechanism of dye-sensitized solar cells. Journal of Physical Chemistry Letters 5:4285–4290. https://doi.org/10.1021/jz502197b

111. Yan W, Xiang F, Ou J, et al (2024) Highly efficient dye-sensitized solar cells achieved by matching energy levels between pseudohalogen redox couples and organic donor−π−acceptor cyanoacrylic acid dyes. Electrochim Acta 473:1–10. https://doi.org/10.1016/j.electacta.2023.143522

112. Hailu YM, Nguyen MT, Jiang JC (2020) Theoretical study on the interaction of iodide electrolyte/organic dye with the TiO2surface in dye-sensitized solar cells. Physical Chemistry Chemical Physics 22:26410–26418. https://doi.org/10.1039/d0cp02532a

113. Andualem A, Demiss S (2018) Review on Dye-Sensitized Solar Cells (DSSCs). Journal of Heterocyclics 1:29–34. https://doi.org/10.33805/2639-6734.103

114. Grätzel M (2005) Solar energy conversion by dye-sensitized photovoltaic cells. Inorg Chem 44:6841–6851. https://doi.org/10.1021/ic0508371

115. Pourebrahimi S, Pirooz M (2024) Exploring the optoelectronic properties of Flavylium cations as acceptors in organic solar Cells: DFT/TD-DFT investigations. Solar Energy 275:1-11. https://doi.org/10.1016/j.solener.2024.112617

116. El Mouhi R, Slimi A, Fitri A, et al (2022) DFT, DFTB and TD-DFT theoretical investigations of π-conjugated molecules based on thieno[2,3-b] indole for dye-sensitized solar cell applications. Physica B Condens Matter 636:1–13. https://doi.org/10.1016/j.physb.2022.413850

117. Xu Z, Li Y, Zhang W, et al (2019) DFT/TD-DFT study of novel T shaped phenothiazine-based organic dyes for dye-sensitized solar cells applications. Spectrochim Acta A Mol Biomol Spectrosc 212:272–280. https://doi.org/10.1016/j.saa.2019.01.002

118. El-Meligy AB, Koga N, Iuchi S, et al (2018) DFT/TD-DFT calculations of the electronic and optical properties of bis-N,N-dimethylaniline-based dyes for use in dye-sensitized solar cells. J Photochem Photobiol A Chem 367:332–346. https://doi.org/10.1016/j.jphotochem.2018.08.036

119. AL-Temimei FA, Omran Alkhayatt AH (2020) A DFT/TD-DFT investigation on the efficiency of new dyes based on ethyl red dye as a dye-sensitized solar cell light-absorbing material. Optik (Stuttg) 208:1–7. https://doi.org/10.1016/j.ijleo.2019.163920

120. Khlaifia D, Chemek M, Alimi K (2020) DFT/TDDFT approach: an incredible success story in prediction of organic materials properties for photovoltaic application. Moroccan Journal of Chemistry 8:683–699. https://doi.org/10.48317/IMIST.PRSM/morjchem-v8i3.18518

121. Setsoafia DDY, Ram KS, Mehdizadeh-Rad H, et al (2022) DFT and TD-DFT Calculations of Orbital Energies and Photovoltaic Properties of Small Molecule Donor and Acceptor Materials Used in Organic Solar Cells. J Renew Mater 10:2553–2567. https://doi.org/10.32604/jrm.2022.020967

122. Sikiru S, Oladosu TL, Amosa TI, et al (2022) Recent advances and impact of phase change materials on solar energy: A comprehensive review. J Energy Storage 53:1–20. https://doi.org/10.1016/j.est.2022.105200

123. Tan CH, Zhang J, Jia T, et al (2023) The Role of Device Mobility on the Charge Generation Process in Polymerized Small-Molecule Acceptor Based Organic Solar Cells. Journal of Physical Chemistry C 127:12135–12142. https://doi.org/10.1021/acs.jpcc.3c02104

124. Brédas JL, Norton JE, Cornil J, Coropceanu V (2009) Molecular understanding of organic solar cells: The challenges. Acc Chem Res 42:1691–1699. https://doi.org/10.1021/ar900099h

125. Ragoussi ME, Torres T (2015) Organic photovoltaics. Revista Virtual de Quimica 7:112–125. https://doi.org/10.5935/1984-6835.20150007

126. Hedström S, Henriksson P, Wang E, et al (2014) Light-harvesting capabilities of low band gap donor-acceptor polymers. Physical Chemistry Chemical Physics 16:24853–24865. https://doi.org/10.1039/c4cp03191a

127. Sahu H, Ma H (2019) Unraveling Correlations between Molecular Properties and Device Parameters of Organic Solar Cells Using Machine Learning. Journal of Physical Chemistry Letters 10:7277–7284. https://doi.org/10.1021/acs.jpclett.9b02772

128. Sahu H, Rao W, Troisi A, Ma H (2018) Toward Predicting Efficiency of Organic Solar Cells via Machine Learning and Improved Descriptors. Adv Energy Mater 8:1–9. https://doi.org/10.1002/aenm.201801032

129. Li X, Zhang Q, Yu J, et al (2022) Mapping the energy level alignment at donor/acceptor interfaces in non-fullerene organic solar cells. Nat Commun 13:1–9. https://doi.org/10.1038/s41467-022-29702-w

130. Oehzelt M, Akaike K, Koch N, Heimel G (2015) Computer Modeling: Energy-level alignment at organic heterointerfaces. Sci Adv 1:1–8. https://doi.org/10.1126/sciadv.1501127

131. Zhang J, Liu W, Zhou G, et al (2020) Accurate Determination of the Minimum HOMO Offset for Efficient Charge Generation using Organic Semiconducting Alloys. Adv Energy Mater 10:1–8. https://doi.org/10.1002/aenm.201903298

132. Wang L, Zhang C, Su Z, et al (2023) Near 0 eV HOMO offset enable high-performance nonfullerene organic solar cells with large open circuit voltage and fill factor. J Mater Chem C 11:6971–6980. https://doi.org/10.1039/D3TC00547J

133. Liu W, Zhang J, Xu S, Zhu X (2019) Efficient organic solar cells achieved at a low energy loss. Sci Bull (Beijing) 64:1144–1147. https://doi.org/10.1016/j.scib.2019.07.005

134. Zhang J, Liu W, Zhang M, et al (2019) Revealing the Critical Role of the HOMO Alignment on Maximizing Current Extraction and Suppressing Energy Loss in Organic Solar Cells. iScience 19:883–893. https://doi.org/10.1016/j.isci.2019.08.038

135. Kraner S, Scholz R, Plasser F, et al (2015) Exciton size and binding energy limitations in one-dimensional organic materials. Journal of Chemical Physics 143:1–7. https://doi.org/10.1063/1.4938527

136. News R, Brédas J-L, Cornil J, Heeger AJ (1996) The Exciton Binding Energy in Luminescent Conjugated Polymers. Ad. Mater. 8:447–452. https://doi.org/10.1002/adma.19960080517

137. Shuai Z, Pati SK, Su WP, et al (1997) Binding energy of 1Bu singlet excitons in the one-dimensional extended Hubbard-Peierls model. Phys Rev B 55:368–371. https://doi.org/10.1103/PhysRevB.55.15368

138. Sun H, Hu Z, Zhong C, et al (2016) Quantitative Estimation of Exciton Binding Energy of Polythiophene-Derived Polymers Using Polarizable Continuum Model Tuned Range-Separated Density Functional. Journal of Physical Chemistry C 120:8048–8055. https://doi.org/10.1021/acs.jpcc.6b01975

139. Knupfer M (2003) Exciton binding energies in organic semiconductors. Appl Phys A Mater Sci Process 77:623–626. https://doi.org/10.1007/s00339-003-2182-9

140. Zhu L, Yi Y, Chen L, Shuai Z (2008) Exciton Binding Energy of Electronic Polymers: A First Principles Study. J Theor Comput Chem 11:517–530. https://doi.org/10.1142/S0219633608003939

141. Zhu L, Wei Z, Yi Y (2022) Exciton Binding Energies in Organic Photovoltaic Materials: A Theoretical Perspective. Journal of Physical Chemistry C 126:14–21. https://doi.org/10.1021/acs.jpcc.1c08898

142. Kashani S, Rech JJ, Liu T, et al (2024) Exciton Binding Energy in Organic Polymers: Experimental Considerations and Tuning Prospects. Adv Energy Mater 14:1–15. https://doi.org/10.1002/aenm.202302837

143. Bredas JL (2014) Mind the gap! Mater Horiz 1:17–19. https://doi.org/10.1039/c3mh00098b

144. Kraner S, Scholz R, Koerner C, Leo K (2015) Design Proposals for Organic Materials Exhibiting a Low Exciton Binding Energy. Journal of Physical Chemistry C 119:22820–22825. https://doi.org/10.1021/acs.jpcc.5b07097

145. Nayak PK (2013) Exciton binding energy in small organic conjugated molecule. Synth Met 174:42–45. https://doi.org/10.1016/j.synthmet.2013.04.010

146. Dkhissi A (2011) Excitons in organic semiconductors. Synth Met 161:1441–1443. https://doi.org/10.1016/j.synthmet.2011.04.003

147. Elumalai NK, Uddin A (2016) Open circuit voltage of organic solar cells: An in-depth review. Energy Environ Sci 9:391–410. https://doi.org/10.1039/c5ee02871j

148. Marinova N, Valero S, Delgado JL (2017) Organic and perovskite solar cells: Working principles, materials and interfaces. J Colloid Interface Sci 488:373–389. https://doi.org/10.1016/j.jcis.2016.11.021

149. Arno Smets, René van Swaaij, Klaus Jäger, et al (2016) Solar energy The physics and engineering of photovoltaic conversion, technologies and systems. UIT Cambridge.

150. Nelson J, Kirkpatrick J, Ravirajan P (2004) Factors limiting the efficiency of molecular photovoltaic devices. Phys Rev B Condens Matter Mater Phys 69:1–11. https://doi.org/10.1103/PhysRevB.69.035337

151. Vandewal K, Tvingstedt K, Gadisa A, et al (2009) On the origin of the open-circuit voltage of polymer-fullerene solar cells. Nat Mater 8:904–909. https://doi.org/10.1038/nmat2548

152. Potscavage WJ, Yoo S, Kippelen B (2008) Origin of the open-circuit voltage in multilayer heterojunction organic solar cells. Appl Phys Lett 93:1–4. https://doi.org/10.1063/1.3027061

153. Qi B, Zhou Q, Wang J (2015) Exploring the open-circuit voltage of organic solar cells under low temperature. Sci Rep 5:1–10. https://doi.org/10.1038/srep11363

154. Scharber MC, Mühlbacher D, Koppe M, et al (2006) Design rules for donors in bulk-heterojunction solar cells - Towards 10 % energy-conversion efficiency. Advanced Materials 18:789–794. https://doi.org/10.1002/adma.200501717

155. Niinomi T, Matsuo Y, Hashiguchi M, et al (2009) Penta(organo)[60]fullerenes as acceptors for organic photovoltaic cells. J Mater Chem 19:5804–5811. https://doi.org/10.1039/b904485j

156. Asbury JB, Wang Y-Q, Hao E, et al (2001) Evidences of hot excited state electron injection from sensitizer molecules to TiO2 nanocrystalline thin films. Res Chem Intermed 27:393–406. https://doi.org/10.1163/156856701104202255

157. Padilla M, Michl B, Thaidigsmann B, et al (2014) Short-circuit current density mapping for solar cells. Solar Energy Materials and Solar Cells 120:282–288. https://doi.org/10.1016/j.solmat.2013.09.019

158. Hartnagel P, Kirchartz T (2020) Understanding the Light-Intensity Dependence of the Short-Circuit Current of Organic Solar Cells. Adv Theory Simul 3:1–11. https://doi.org/10.1002/adts.202000116

159. Lu N, Li L, Sun P, Liu M (2014) Short-circuit current model of organic solar cells. Chem Phys Lett 614:27–30. https://doi.org/10.1016/j.cplett.2014.08.070

160. (2020) ASTM Standard G173-03. Standard Tables for Reference Solar SpectralIrradiances: Direct Normal and Hemispherical on 37° Tilted Surface. In: ASTM International. https://www.astm.org/g0173-03r20.html Accessed 15 Dec 2024

161. Bérubé N, Gosselin V, Gaudreau J, Côté M (2013) Designing polymers for photovoltaic applications using ab initio calculations. Journal of Physical Chemistry C 117:7964–7972. https://doi.org/10.1021/jp309800f

162. Feng J, Jiao Y, Ma W, et al (2013) First principles design of dye molecules with ullazine donor for dye sensitized solar cells. Journal of Physical Chemistry C 117:3772–3778. https://doi.org/10.1021/jp310504n

163. Han G, Yi Y (2022) Molecular Insight into Efficient Charge Generation in Low-Driving-Force Nonfullerene Organic Solar Cells. Acc Chem Res 55:869–877. https://doi.org/10.1021/acs.accounts.1c00742

164. Nakano K, Chen Y, Xiao B, et al (2019) Anatomy of the energetic driving force for charge generation in organic solar cells. Nat Commun 10:1–10. https://doi.org/10.1038/s41467-019-10434-3

165. Coffey DC, Larson BW, Hains AW, et al (2012) An optimal driving force for converting excitons into free carriers in excitonic solar cells. Journal of Physical Chemistry C 116:8916–8923. https://doi.org/10.1021/jp302275z

166. Lüer L, Wang R, Liu C, et al (2024) Maximizing Performance and Stability of Organic Solar Cells at Low Driving Force for Charge Separation. Advanced Science 11:1–20. https://doi.org/10.1002/advs.202305948

167. Ward AJ, Ruseckas A, Kareem MM, et al (2015) The impact of driving force on electron transfer rates in photovoltaic donor-acceptor blends. Advanced Materials 27:2496–2500. https://doi.org/10.1002/adma.201405623

168. Yang W, Yao Y, Guo P, et al (2018) Optimum driving energy for achieving balanced open-circuit voltage and short-circuit current density in organic bulk heterojunction solar cells. Physical Chemistry Chemical Physics 20:29866–29875. https://doi.org/10.1039/c8cp05145c

169. Liu J, Chen S, Qian D, et al (2016) Fast charge separation in a non-fullerene organic solar cell with a small driving force. Nat Energy 1:1-7. https://doi.org/10.1038/nenergy.2016.89

170. Sun LL, Zhang T, Wang J, et al (2015) Exploring the influence of electron donating/withdrawing groups on hexamolybdate-based derivatives for efficient p-

type dye-sensitized solar cells (DSSCs). RSC Adv 5:39821–39827. https://doi.org/10.1039/c5ra05164a

171. Xu Z, Lu X, Li Y, Wei S (2020) Theoretical analysis on heteroleptic Cu(I)-based complexes for dye-sensitized solar cells: Effect of anchors on electronic structure, spectrum, excitation, and intramolecular and interfacial electron transfer. Molecules 25:1-15. https://doi.org/10.3390/molecules25163681

172. Megala M, Rajkumar BJM (2016) Theoretical study of anthoxanthin dyes for dye sensitized solar cells (DSSCs). J Comput Electron 15:557–568. https://doi.org/10.1007/s10825-016-0791-8

173. Benesperi I, Michaels H, Freitag M (2018) The researcher's guide to solid-state dye-sensitized solar cells. J Mater Chem C Mater 6:11903–11942. https://doi.org/10.1039/C8TC03542C

174. Keremane KS, Abdellah IM, Naik P, et al (2020) Simple thiophene-bridged D-π-A type chromophores for DSSCs: a comprehensive study of their sensitization and co-sensitization properties. Physical Chemistry Chemical Physics 22:23169–23184. https://doi.org/10.1039/d0cp02781b

175. Zhang ZL, Zou LY, Ren AM, et al (2013) Theoretical studies on the electronic structures and optical properties of star-shaped triazatruxene/heterofluorene co-polymers. Dyes and Pigments 96:349–363. https://doi.org/10.1016/j.dyepig.2012.08.020

176. Oliveira EF, Lavarda FC (2016) Reorganization energy for hole and electron transfer of poly(3-hexylthiophene) derivatives. Polymer (Guildf) 99:105–111. https://doi.org/10.1016/j.polymer.2016.07.003

177. Poelking Carl and Daoulas K and TA and AD (2014) Morphology and Charge Transport in P3HT: A Theorist's Perspective. In: Ludwigs S (ed) P3HT Revisited – From Molecular Scale to Solar Cell Devices. Springer Berlin Heidelberg, Berlin, Heidelberg, pp 139–180

178. García G, Moral M, Garzón A, et al (2012) Poly(arylenethynyl-thienoacenes) as candidates for organic semiconducting materials. A DFT insight. Org Electron 13:3244–3253. https://doi.org/10.1016/j.orgel.2012.09.029

179. Hutchison GR, Ratner MA, Marks TJ (2005) Hopping transport in conductive heterocyclic oligomers: Reorganization energies and substituent effects. J Am Chem Soc 127:2339–2350. https://doi.org/10.1021/ja0461421

180. Parr RG, Pearson RG (1983) Absolute Hardness: Companion Parameter to Absolute Electronegativity. J Am Chem Soc 105:7512–7516. https://doi.org/10.1021/ja00364a005

181. Pearson RG (1986) Absolute electronegativity and hardness correlated with molecular orbital theory. Proc Nati Acad Sci USA 83:8440–8441. https://doi.org/10.1073/pnas.83.22.8440

182. Idrissi A, Elfakir Z, Atir R, Bouzakraoui S (2023) Small thiophene-based molecules with favorable properties as HTMs for perovskite solar cells or as active materials in organic solar cells. Journal of Physics and Chemistry of Solids 181:1-7. https://doi.org/10.1016/j.jpcs.2023.111492

183. Delgado-Montiel T, Baldenebro-López J, Soto-Rojo R, Glossman-Mitnik D (2016) Quantum chemical study of the effect of π-bridge on the optical and electronic properties of sensitizers for DSSCs incorporating dioxythiophene and thiophene units. Theor Chem Acc 135:1-10. https://doi.org/10.1007/s00214-016-1989-3

184. Arunkumar A, Deepana M, Shanavas S, et al (2019) Computational Investigation on Series of Metal-Free Sensitizers in Tetrahydroquinoline with Different π-spacer Groups for DSSCs. ChemistrySelect 4:4097–4104. https://doi.org/10.1002/slct.201803961

185. Soto-Rojo R, Baldenebro-López J, Glossman-Mitnik D (2015) Study of chemical reactivity in relation to experimental parameters of efficiency in coumarin derivatives for dye sensitized solar cells using DFT. Physical Chemistry Chemical Physics 17:14122–14129. https://doi.org/10.1039/c5cp01387a

186. Delgado-Montiel T, Baldenebro-López J, Soto-Rojo R, Glossman-Mitnik D (2020) Theoretical study of the effect of π-bridge on optical and electronic properties of carbazole-based sensitizers for DSSCs. Molecules 25:1-17 . https://doi.org/10.3390/molecules25163670

187. Chattaraj PK, Roy DR (2007) Electrophilicity index. Chem Rev 107:46–74. https://doi.org/10.1021/cr078014b

188. Gázquez JL, Cedillo A, Vela A (2007) Electrodonating and electroaccepting powers. Journal of Physical Chemistry A 111:1966–1970. https://doi.org/10.1021/jp065459f

189. Afolabi SO, Semire B, Akiode OK, Idowu MA (2022) Quantum study on the optoelectronic properties and chemical reactivity of phenoxazine-based organic photosensitizer for solar cell purposes. Theor Chem Acc 141:1-14. https://doi.org/10.1007/s00214-022-02882-w

190. Parr RG, Donnelly RA, Levy M, Palke WE (1977) Electronegativity: The density functional viewpoint. J Chem Phys 68:3801–3807. https://doi.org/10.1063/1.436185

191. Constantin CP, Damaceanu MD, Mihaila M, Kusko M (2022) Open-Circuit Voltage Degradation by Dye Mulliken Electronegativity in Multi-Anchor Organic Dye-Based Dye-Sensitized Solar Cells. ACS Appl Energy Mater 5:7600–7616. https://doi.org/10.1021/acsaem.2c01059

192. Phillips JC (1961) Generalized Koopmans' Theorem*. Phisical Review 123:420–424. https://doi.org/10.1103/PhysRev.123.420

193. Tsuneda T, Song JW, Suzuki S, Hirao K (2010) On Koopmans' theorem in density functional theory. Journal of Chemical Physics 133:. https://doi.org/10.1063/1.3491272

194. Koopmans YT (1934) Uber Die Zuordnung Von Wellenfunk-Tionen Und Eigenwerten Zu Den, Einzelnen Elektronen Eines Atoms. Physica 1–6. https://doi.org/10.1016/S0031-8914(34)90011-2

195. Becke AD (1993) Density-functional thermochemistry. III. The role of exact exchange. J Chem Phys 98:5648–5652. https://doi.org/10.1063/1.464913

196. Khadiri A, Warad I, Abuelizz HA, et al (2024) Predicting photovoltaic parameters using DFT and TD-DFT calculations of novel triphenylamine-based organic dyes: The effect of the internal or auxiliary acceptors on photovoltaic

performance for DSSC. Solar Energy 279:1-22. https://doi.org/10.1016/j.solener.2024.112832

197. Akram W, Walayat A, Zahid WA, et al (2024) Rational Design and Engineering of Terminal Functional Groups in Dibenzothiophene-Diphenylamine Small Molecular Electron Donors for Enhanced Photovoltaic Efficiency in All-Small-Molecule Organic Solar Cells. Adv Theory Simul 7:1-22. https://doi.org/10.1002/adts.202400289

198. Pourebrahimi S, Pirooz M (2024) Exploring the optoelectronic properties of Flavylium cations as acceptors in organic solar Cells: DFT/TD-DFT investigations. Solar Energy 275:1–11. https://doi.org/10.1016/j.solener.2024.112617

199. Khadiri A, Warad I, Abuelizz HA, et al (2024) Predicting photovoltaic parameters using DFT and TD-DFT calculations of novel triphenylamine-based organic dyes: The effect of the internal or auxiliary acceptors on photovoltaic performance for DSSC. Solar Energy 279:1-22. https://doi.org/10.1016/j.solener.2024.112832

200. Shafiq F, Mubarik A, Rafiq M, Alshehri SM (2024) Star-shaped small donor molecules based on benzotriindole for efficient organic solar cells: a DFT study. J Mol Model 30:1-14. https://doi.org/10.1007/s00894-024-05870-y

201. Bourass M, Benjelloun AT, Benzakour M, et al (2016) DFT and TD-DFT calculation of new thienopyrazine-based small molecules for organic solar cells. Chem Cent J 10:1-11. https://doi.org/10.1186/s13065-016-0216-6

202. Brédas JL (2017) Organic Electronics: Does a Plot of the HOMO-LUMO Wave Functions Provide Useful Information? Chemistry of Materials 29:477–478. https://doi.org/10.1021/acs.chemmater.6b04947

203. Bursch M, Mewes J-M, Hansen A, Grimme S (2022) Best-Practice DFT Protocols for Basic Molecular Computational Chemistry. 134: 1-27. https://doi.org/10.26434/chemrxiv-2022-n304h

204. Zhang G, Musgrave CB (2007) Comparison of DFT methods for molecular orbital eigenvalue calculations. Journal of Physical Chemistry A 111:1554–1561. https://doi.org/10.1021/jp061633o

205. Zhou B, Hu Z, Jiang Y, et al (2018) Benchmark study of ionization potentials and electron affinities of armchair single-walled carbon nanotubes using density functional theory. Journal of Physics Condensed Matter 30:1-11. https://doi.org/10.1088/1361-648X/aabd18

206. Kronik L, Stein T, Refaely-Abramson S, Baer R (2012) Excitation gaps of finite-sized systems from optimally tuned range-separated hybrid functionals. J Chem Theory Comput 8:1515–1531. https://doi.org/10.1021/ct2009363

207. Wong BM, Hsieh TH (2010) Optoelectronic and excitonic properties of oligoacenes: Substantial improvements from range-separated time-dependent density functional theory. J Chem Theory Comput 6:3704–3712. https://doi.org/10.1021/ct100529s

208. Rostami Z, Hosseinian A, Monfared A (2018) DFT results against experimental data for electronic properties of C60 and C70 fullerene derivatives. J Mol Graph Model 81:60–67. https://doi.org/10.1016/j.jmgm.2018.02.009

209. Grüning M, Gritsenko O V., Baerends EJ (2003) Exchange-correlation energy and potential as approximate functionals of occupied and virtual Kohn-Sham orbitals: Application to dissociating H2. Journal of Chemical Physics 118:7183–7192. https://doi.org/10.1063/1.1562197

210. Bora SR, Kalita DJ (2024) Molecular engineering of the core part of D-π-A-π-D based small acceptor molecules for efficient organic solar cells: a DFT approach. New Journal of Chemistry 48:10897–10909. https://doi.org/10.1039/d4nj01629g

211. Tommalieh MJ, Aljameel AI, Hussein RK, et al (2024) The Effect of Conjugated Nitrile Structures as Acceptor Moieties on the Photovoltaic Properties of Dye-Sensitized Solar Cells: DFT and TD-DFT Investigation. Int J Mol Sci 25:1-15. https://doi.org/10.3390/ijms25137138

212. Abdali SA, AL-Temimei FA, Al-Abbas SS (2024) Design a New D-π-A Formation Dyes as Dye-sensitized Solar Cells Applications/ a DFT and TD-DFT Study. J Fluoresc 34:795–807. https://doi.org/10.1007/s10895-023-03311-2

213. Mouhi R El, Slimi A, Khattabi S El, et al (2024) Computational study of new small molecules D-A based on triphenylamines for bulk heterojunction solar cells

(BHJ). Comput Theor Chem 1241:1-11. https://doi.org/10.1016/j.comptc.2024.114899

214. Huang Y, Zhang K, Song P, et al (2024) Heterojunction Organic Solar Cells with Efficient Charge Mobility and Separation Capabilities Studied by DFT. Chemistry – A European Journal. 1-17. https://doi.org/10.1002/chem.202402928

215. Praveen PA, Saravanapriya D, Bhat S V., et al (2024) Comprehensive analysis of DFT-3C methods with B3LYP and experimental data to model optoelectronic properties of tetracene. Mater Sci Semicond Process 173:1-8. https://doi.org/10.1016/j.mssp.2024.108159

216. Kumar R, Singh A (2024) Designing of π-Bridge for Metal Free Dye-Sensitized Solar Cell and Optoelectronic Properties: An ab initio DFT Perspective. Chemistry Select 9:1-10. https://doi.org/10.1002/slct.202400526

217. Praveen PA, Saravanapriya D, Bhat S V., et al (2024) Comprehensive analysis of DFT-3C methods with B3LYP and experimental data to model optoelectronic properties of tetracene. Mater Sci Semicond Process 173:1-8. https://doi.org/10.1016/j.mssp.2024.108159

218. Hehre WJ, Ditchfield K, Pople JA (1972) Self-consistent molecular orbital methods. XII. Further extensions of gaussian-type basis sets for use in molecular orbital studies of organic molecules. J Chem Phys 56:2257–2261. https://doi.org/10.1063/1.1677527

219. Tommalieh MJ, Aljameel AI, Hussein RK, et al (2024) The Effect of Conjugated Nitrile Structures as Acceptor Moieties on the Photovoltaic Properties of Dye-Sensitized Solar Cells: DFT and TD-DFT Investigation. Int J Mol Sci 25:1-15. https://doi.org/10.3390/ijms25137138

220. Krishnan R, Binkley JS, Seeger R, Pople JA (1980) Self-consistent molecular orbital methods. XX. A basis set for correlated wave functions. J Chem Phys 72:650–654. https://doi.org/10.1063/1.438955

221. Lopez SA, Pyzer-Knapp EO, Simm GN, et al (2016) The Harvard organic photovoltaic dataset. Sci Data 3:1-7. https://doi.org/10.1038/sdata.2016.86

222. Setsoafia DDY, Ram KS, Mehdizadeh-Rad H, et al (2023) Density Functional Theory Simulation of Optical and Photovoltaic Properties of DRTB-T Donor-Based Organic Solar Cells. Int J Energy Res. 2023:1-12 https://doi.org/10.1155/2023/6696446

223. Weigend F, Ahlrichs R (2005) Balanced basis sets of split valence, triple zeta valence and quadruple zeta valence quality for H to Rn: Design and assessment of accuracy. Physical Chemistry Chemical Physics 7:3297–3305. https://doi.org/10.1039/b508541a

224. Qadir KW, Mohammadi MD, Abbas F, Abdullah HY (2024) Molecular engineering of BTO for superior photovoltaic efficiency: A DFT exploration. Mater Chem Phys 314:1-9. https://doi.org/10.1016/j.matchemphys.2023.128866

225. Tendongmo H, Kogge BF, Tamafo Fouegue AD, et al (2024) Theoretical screening of N-[5′-methyl-3′-isoxasolyl]-N-[(E)-1-(-2-thiophene)] methylidene]amine and its isoxazole based derivatives as donor materials for bulk heterojunction organic solar cells: DFT and TD-DFT investigation. J Mol Model 30:1-16. https://doi.org/10.1007/s00894-024-05978-1

[226] Jin, R. (2015) Theoretical study of the optical and charge transport properties of star-shaped molecules with 1,3,5-triazine-core derivatives as organic light-emitting and organic solar cells materials. C. R. Chim. 18: 954–959. https://doi.org/10.1016/j.crci. 2015.05.021

[227] Vidya, VM, Tripathi, A, Prabhakar, C (2019) Linear, non-linear optical properties and reorganization energies of D- π-A star-shaped triazine derivatives: a DFT study. J. Mol. Struct. 1176:855–864. https://doi.org/10.1016/j.molstruc.2018.09.025

[228] Zhang, H, Zang, XF, Hong, YP, Chen, ZE (2021) Theoretical and photovoltaic investigations of 1,3,5-triazine-based photosensitizers achieving highly efcient DSSCs. Synth. Met. 280:1-7. https://doi.org/10.1016/j.synthmet.2021.116882

[229] Vidya VM, Someshwar, P, Prabhakar, C. (2021) Optoelectronic and charge transport properties of D-n-A type 1,3,5-triazine derivatives: a combined experimental and DFT study. Spectrochim. Acta A Mol. Biomol. Spectrosc. 245:1-13. https://doi.org/10.1016/j.saa.2020.118940